Connectivity in the Yeast Cell Cycle Transcription Network: Inferences from Neural Networks

Christopher E. Hart[1,2], Eric Mjolsness[3,5], Barbara J. Wold[2,4,5]

1 Current Address: Department of Molecular, Cellular, and Developmental Biology, Yale University, New Haven, CT 06405

2 Division of Biology, California Institute of Technology, Pasadena, CA 91125

3 University of California, Irvine, Institute for Genomics and Bioinformatics, School of Information & Computer Science, Irvine, CA 92697,

4 Corresponding Author

5 Caltech Beckman Institute, Biological Network Modelling Center

Abstract

Background: A current challenge is to develop computational approaches to infer gene network regulatory relationships based on multiple types of large-scale functional genomic data.

Methodology/primary findings: We find that single-layer feed-forward Artificial Neural Network (ANN) models can effectively discover gene network structure by integrating global in vivo protein:DNA interaction data (ChIP/Array) with genome-wide microarray RNA data. We test this on the yeast cell cycle transcription network, which is composed of several hundred genes with phase specific RNA outputs. These ANNs were robust to noise in data and to a variety of perturbations. They reliably identified and ranked 10 of 12 known major cell cycle factors at the top of a set of 204, based on a sum-of-squared weights metric. Comparative analysis of motif occurrences among multiple yeast species independently confirmed relationships inferred from ANN weights analysis.

Conclusions/significance: ANN models can capitalize on properties of biological gene networks that other kinds of models do not. ANNs naturally take advantage of patterns of absence, as well as presence, of factor binding associated with specific expression output; they are easily subjected to in silico "mutation" to uncover biological redundancies; and they can use the full range of factor binding values. A prominent feature of cell cycle ANNs suggested an analogous property might exist in the biological network. This postulated "network-local discrimination" occurs when regulatory connections (here between MBF and target genes) are explicitly disfavored in one network module (G2), relative to others and to the class of genes outside the mitotic network. If correct, this predicts that MBF motifs will be significantly depleted from the discriminated class and that the discrimination will persist through evolution. Analysis of distantly related S. pombe confirmed this, suggesting that network-local discrimination is real and complements well–known enrichment of MBF sites in G1 class genes.

1 Introduction

Hundreds of yeast RNAs are expressed in a cell cycle dependent, oscillating manner. In both budding yeast and fission yeast, these RNAs cluster into four or five groups, each corresponding roughly to a phase of the cycle (Spellman et al., 1998; Cho et al., 1998; Rustici et al., 2004; Peng et al., 2004; Oliva et al., 2005; Zhang, 1999; Breeden, 2000; Breeden, 2003; Hart et al., 2005). Large sets of phase specific RNAs are also seen in animal and plant cells (Cho et al., 2001; Whitfield et al., 2002; Menges et al., 2003), arguing that an extensive cycling transcription network is a fundamental property of Eukaryotes. The complete composition and connectivity of the cell cycle transcription network is not yet known for any eukaryote, and many components may vary over long evolutionary distances (Rustici et al., 2004; Peng et al., 2004; Oliva et al., 2005; Bahler, 2005), but some specific regulators (e.g. MBF of yeast and the related E2Fs of plants and animals) are paneukaryotic, as are some of their direct target genes (DNA polymerase, ribonucleotide reductase). Coupled with experimental accessibility, this conservation of core components and connections, make the yeast mitotic cycle an especially good test case for studies of network structure, function and evolution.

To expose the underlying logic of this transcription network, a starting point is to decompose the cell cycle into its component phases (i.e. G1, S, G2, M) and link the pertinent regulatory factors with their immediate regulatory output patterns, here in the form of phasic RNA expression. One way to do this is to integrate multiple genome-wide data types that impinge on connection inference, including factor:DNA interaction data from chromatin IP (ChIP) studies, RNA expression patterns, and comparative genomic analysis. This is appealing partly because these assays are genome-comprehensive and hypothesis independent, so they can, in principle, reveal regulatory relationships not detected by classical genetics. However, the scale and complexity of these datasets require new methods to discover and rank candidate connections, while also accommodating considerable experimental and biological

noise (e.g. (Wang et al., 2002; Bar-Joseph et al., 2003; Luscombe et al., 2004; M. A. Beer, 2004; Lee et al., 2004; Gao et al., 2004; Sun et al., 2006)).

Microarray RNA expression studies in budding yeast have identified 230 to 1100 cycling genes, the upper number encompassing nearly a fifth of all yeast genes ((Spellman et al., 1998; Cho et al., 1998; Breeden, 2003; de Lichtenberg et al., 2005)). Specifics of experimental design and methods of analysis contribute to the wide range in the number of genes designated as cycling, but there is agreement on a core set of nearly 200. Yeast molecular genetic studies have established that transcriptional regulation is critical for controlling phase specific RNA expression for some of these genes, though this does not exclude modulation and additional contributions from post-transcriptional mechanisms. About a dozen Saccharomyces transcription factors have been causally associated with direct control of cell cycle expression patterns, including repressors, activators, co-regulators, and regulators that assume both repressing and activating roles, depending on context: Ace2, Fkh1, Fkh2, Mbp1, Mcm1, Ndd1, Stb1, Swi4, Swi5, Swi6, Yhp1, and Yox1.

These can serve as internal control true-positive connections. Conversely, a majority of yeast genes have no cell cycle oscillatory expression, and true negatives can be drawn from this group. A practical consideration is how well the behavior of a network is represented in critical datasets. In this case, cells in all cell cycle phases are present in the mixed phase, exponentially growing yeast cultures used for the largest and most complete set of global protein:DNA interaction (ChIP/array) data so far assembled in functional genomics ((Harbison et al., 2004)). These data are further supported by three smaller studies of the same basic design (Horak et al., 2002; Iyer et al., 2001; Lee et al., 2002). This sets the cell cycle apart from many other transcription networks whose multiple states are either partly or entirely absent from the global ChIP data. Equally important are RNA expression data that finely parse the kinetic trajectory for every gene across the cycle of budding yeast (Cho et al., 1998; Spellman et al., 1998)

and also in the distantly related fission yeast, S. pombe (Rustici et al., 2004; Peng et al., 2004; Oliva et al., 2005). This combination of highly time-resolved RNA expression data and phase-mixed (but nevertheless inclusive) ChIP/array data can be used to assign protein:DNA interactions to explicit cell cycle phases, while evolutionary comparison with *S. pombe* highlight exceptionally conserved and presumably fundamental network properties.

Many prior efforts to infer yeast transcription network connections from genome-wide data (Bar-Joseph et al., 2003; Segal et al., 2003b; Tsai et al., 2005; Luscombe et al., 2004; M. A. Beer, 2004)) were designed to address the global problem of finding connection patterns across the entire yeast transcriptiome by using very large and diverse collections of yeast RNA, DNA and/or chromatin immunoprecipitation data. The present work focuses instead on a single cellular process and its underlying gene network, which represents a natural level of organization positioned between the single gene at one extreme and the entire interlocking community of networks that govern the entire cell.

To model regulatory factor: target gene behavior, we adapt neural networks and use them to integrate global expression and protein:DNA interaction data.

Artificial neural networks (ANNs) are structural computational models with a long history in pattern recognition (Bishop, 1995). A general reason for thinking ANNs could be effective for this task is that they have some natural similarities with transcription networks, including the ability to create non-linear sparse interactions between transcriptional regulators and target genes. They have previously been applied previously to model relatively small gene circuits (Mjolsness et al., 1991; Weaver et al., 1999; Vohradsky, 2001), though they have not, to our knowledge, been used for the problem of inferring network structure by integrating large-scale data. We reasoned that a simple single layer ANN would be well suited to capture and leverage two additional known characteristics of eukaryotic gene networks. First, factor binding *in vivo* varies over a continuum of values, as reflected in ChIP

data, *in vivo* footprinting, binding site numbers and affinity ranges, and site mutation analyses. These quantitative differences can have biological significance to transcription output by affecting cooperativity, background "leaky expression" or the lack of it, and the temporal sequencing of gene induction as factors become available or disappear. This is quite different from a world in which binding is reduced to a simple two state, present/absent call. Neural networks are able to use the full range of binding probabilities in the dataset. Second, ANNs can give weight and attention to structural features such as the persistent absence of specific factors from particular target groups of genes. This “negative image” information is not recovered and used by other methods applied to date ((Harbison et al., 2004; Bar-Joseph et al., 2003; Sun et al., 2006; Workman et al., 2006)). The inherent ability of ANNs to use these properties is a potential strength compared with algorithms that rest solely on positive evidence of factor:target binding or require discretization of binding measurements into a simplified bound/unbound call.

ANNs have been most famously used in machine learning as "black boxes" to perform classification tasks, in which the goal is to build a network based on a training dataset that will subsequently be used to perform similar classifications on new data of similar structure. In these classical ANN applications, the weights within the network are of no particular interest, as long as the trained network performs the desired classification task successfully when extrapolating to new data. ANNs are used here in a substantially different way, serving as structural models (Reinitz et al., 1995). Specifically, we use simple feed-forward networks in which the results of interest are mainly in the weights and what they suggest about the importance of individual transcription factors or groups of factors for specifying particular expression outputs.

Here ANNs were trained to predict the RNA expression behavior of genes during a cdc28 synchronized cell cycle, based solely on transcription factor binding pattern, as measured by ChIP/array for

204 yeast factors determined in an exponentially growing culture (Harbison et al., 2004). The resulting ANN model is then interrogated to identify the most important regulator-to-target gene associations, as reflected by ANN weights. Ten of the twelve major known transcriptional regulators of cell cycle phase specific expression ranked at the very top of the 204-regulator list in the model. The cell cycle ANNs were remarkably robust to a series of in silico “mutations”, in which binding data for a specific factor was eliminated and a new family of ANN models were generated. Additional doubly and triply "mutated" networks correctly identified epistasis relationships and redundancies in the biological network. This approach was also applied to two additional, independent cell cycle expression studies to illustrate generality across data platforms, and to probe how the networks might change under distinct modes of cell synchronization.

Analysis of the weights matrices from the resulting models shows that the neural nets take advantage of information about specifically disfavored or disallowed connections between factors and expression patterns, together with the expected positive connections (and weights) for other factors, to assign genes to their correct expression outputs. This led us to ask if there is a corresponding bias in the biological network against binding sites for specific factors in some expression families as suggested by the ANN. We found that this is the case, in multiple *sensu stricto* yeast genomes relatively closely related to *S. cerevisiae*, and also in the distantly related fission yeast, *S. pombe*. This appears to be a deeply conserved network architecture property, even though very few specific orthologous genes are involved.

2 Results

Classifier artificial neural networks (ANNs) were trained to predict membership in cell cycle phase specific RNA clusters, based on global transcription factor binding data (figure 1). As expression input

data, these ANNs used time course microarray data (Cho et al., 1998) for 384 cycling genes that had been grouped into five clusters by an expectation maximization (EM) algorithm (Hart et al., 2005). As measured by receiver operator characteristic (ROC) analysis, these clusters are quantitatively well separated from each other, with less than 10% overlap at their margins with any other clusters, except that the S-phase cluster (EM3) was somewhat less well-separated from its kinetic neighbors, EM2 and EM4 (Hart et al., 2005). The primary goal of the ANN modeling is to infer the set of regulatory connections that underlies each of the cell cycle phased expression groups. Note that a given cluster might be composed of more than one regulatory subgroup; it need not be the case that all associated regulators interact with all–or even most–of the genes in a cluster. ANNs were trained to assign expression cluster membership for each gene based on 204 measured binding probabilities from ChIP/array experiments (Harbison et al., 2004). To accommodate the scarcity of data, while minimizing effects of overtraining, we generated an average-of-bests artificial neural network (aobANN) (Materials and Methods). As anticipated, the aobANN classified input genes best, correctly assigning the expression class of 86% of included cell cycle genes (figure 2). Individual best-of-ten networks, each trained on 80% of the data and tested on the remaining 20% correctly assigned expression class membership for 50% of the genes, with an accuracy range between 40% and 65%, where as only 27% of genes would be expected to be classified correctly if genes were classified by a random process (supplemental figure 1). As shown in supplemental information (supplemental figure 4), a substantial fraction of genes (32%) are always classified correctly by every ANN, another subset (28%) are never classified "correctly", and the remaining fraction (40%) are intermediate. An examination of possible correlates of high or low predictability, including absolute level of RNA expression and bidirectional versus unidirectional orientation of the a gene relative to its upstream neighbor found no correlation except that the EM2 (late G1) class is enriched in highly predictable genes, while the EM5 (M phase expression peak) is

most impoverished (supplemental figure 4). The major conclusion from global statistics is that individual ANNs and the aobANN have developed weighting schemes that are effective in connecting factor binding information from ChIP/array to RNA expression patterns, even in the presence of considerable experimental noise that is a widely acknowledged property of the input datasets.

2.1 Parsing the ANN Weight Matrix to Infer Regulatory Relationships

We next interrogated the aobANN weight matrix to find out which regulators are most important for assigning genes to specific gene expression behavior. Regulators were sorted by a sum-of-squares rank calculation (see methods) over of the expression classes. The factor ranking, based exclusively on the ANN weights, assigned nearly all transcription factors previously definitively associated with phase specific regulation to the very top of the ordered list. Figures 3 and 5 summarize data from the weight matrix of the average-of-bests network. A plot of the sum of squared weights for each factor, shows that the top 10% of all regulators carry much higher weights than all the rest, and the drop off in weight is quite dramatic (figure 3a). Focusing on the top 20%, the relative contribution to each sum derived from positive (blue) versus negative (red) weights is shown (figure 3b). Both negative and positive weights contribute substantially, and the way in which weights associate with each individual expression class is shown in figure 3B. The top regulators in this ranking are Swi6, Ndd1, Stb1, Fkh2, and Mbp1, all of which are known direct regulators of the cell cycle. In most instances high positive weight for a factor (blue) is associated with the expression class or pair of classes expected from more detailed molecular genetics studies. For instance, Swi6, Stb1 and Mbp1 are the first, second and sixth ranked regulators, and they are known to function together at genes expressed in EM2 (G1). Mbp1 binds DNA directly and Swi6 and Stb1 bind to Mbp1 (Koch et al., 1993; Costanzo et al., 2003). Ndd1 and Fkh2, the second and fourth ranked regulators, also function together in a molecular complex (Koranda et al., 2000). In

the aobANN model, they are associated with EM3/4 (S/G2), again recapitulating expected domain of action.

2.2 ANN Stability

Regulator-to-target relationships suggested by the ANNs were very stable with respect to permutation of the input DNA binding data and to a range of biologically reasonable differences among input expression clusterings (classifications). We find the relative ranking of the top regulators to be stable across all networks generated during the training paradigm (figure 4). The ranking of regulators was also stable across networks that were trained to predict expression classes derived from clusterings with either more or fewer clusters (the experiment was performed over K= 5,6,7, or 8 and results are summarized in supplemental figure 2. Lower K values than 4 fit the data poorly and are therefore irrelevant; and still higher K values than 7 force an entirely unjustified over-splitting of clusters that is clearly inappropriate.

2.3 In silico network mutations

We next performed a series of in silico network mutations in which binding data for one, two or three top-ranked regulators were removed before training a new set ANNs. The resulting deletion ANNs were used to produce a new average-of-bests network, as before, and the corresponding sum of squared weights ranking was constructed (figure 6). These perturbations further test network stability and also identify specific instances of factor redundancy. Overall the ANNs proved remarkably stable to elimination of high-ranking factors. When each of the top 20 were eliminated singly, the identity of the remaining top regulators proved very stable (Figure 6a). The color code for each cell reflects its rank order from the parental, unperturbed network (shown in the bottom row). Each subsequent row

reports the outcome for the mutant network with the indicated factor or factors removed. Although the cells are placed according to their rank order in the mutant AOB network, the color is based on the ranking from the unperturbed, “wildtype” network. In general, factors from lower rankings were not promoted into the high ranking (dark blue) domain, nor were previously highly ranked factors (blue) demoted significantly into yellow and red domains. Thus the first major conclusion from the mutation experiments is that neither the connections the ANNs infer, nor the absolute performance of the ANNs depend heavily on a single factor or even a factor pair. The ability of the models to highlight other important connections is not compromised by elimination any high scoring factor.

Panel b in figure 6 shows the same mutant networks at higher resolution, so that all factors whose original rank was >50 appear in the summary as white cells. Original rank order is again indicated by the color of each cell, although the color scale has been shifted to make it more sensitive to changes in rank among the top 50 regulators. A few specific exceptions to overall stability were observed, in which a relatively low ranked regulator has been elevated by mutation into higher ranks. The most striking example is Swi4, which is demarcated with a star. Swi4 is a very well-studied cell cycle transcription factor that did not fall in the top 10% in the wild-type network (it ranked 80th). As shown in panel C, “mutant” networks for all factors associated with the G1 (EM2) caused Swi4 to advance in rank, with double or triple mutations moving it progressively higher. We discuss later the causes and consequences of Swi4’s initial low ranking in the wildtype ANN and the implicates for detecting biological redundancy. However, the general conclusion for ANN analysis is that systematic single and multiple perturbations of high ranking regulators provides a way to detect redundancy, even when a connection - here Swi4 with G1 - was not evident in the unperturbed "wildtype" ANN. Additional double and triple mutations for the major cycle classes were performed and no other change as remarkable as Swi4 was found.

2.4 Out-of-sample accuracy

We next tested out-of-sample accuracy, which is the ability of the training paradigm to generalize to another set of independently collected binding measurements, in which both experimental error and biological error will differ from the first series of models. We constructed a new aobANN trained again from data collected from Harbison, but included only binding measurements from the 111 regulators available in both the Harbison et al. (2004) study and the independent Lee et al. (2002) study. Despite biological and experimental difference between the two datasets, this aobANN delivered a highly significant out of sample accuracy of 56%, which is 17 standard deviations from the average linear assignment score ($.27 \pm 0.017$) of a random partitioning of the genes, where class sizes are determined by drawing from a multinomial distribution based on the cluster sizes.

2.5 Regulator Rank Stability and Power

The stability of weight ranks across the 40 individual "best" networks that contribute to the aobANN was examined. We postulated that factors whose rankings are less stable across many individual networks would also be less likely to be functionally significant than factors showing high stability across the individual networks, even if the median sum-of-squares weight is quite high in all cases. The well known regulators of cell cycle transcription, ranking in the top dozen showed greatest stability, and a substantial discontinuity was found to separate the top 20 from the remaining factors (Figure 4). We then asked how well the top regulators can perform if they are used to build a new aobANN over a sweep that ranges from three to 28 regulators. This experiment showed that a network built from the top 20 regulators performed almost as well as the full 204 regulator network and ranked its regulators very similarly (Supplemental figure 3). The top 5 regulators on their own (Swi6/Mbp1/Stb1 plus Fkh2and Ndd1) were surprisingly powerful in parsing G1 vs. G2/M. Conversely, an aobANN composed from

the bottom 184 regulators was much less successful in predicting expression.

2.6 ANN models from independent cell cycle experiments

We next independently clustered Cdc15 TS and alpha factor synchronized cell cycle RNA expression data (Spellman et al., 1998), and used these new clusters to build two new ANN cell cycle models. These datasets are from two different cell cycle experiments, each measured using deposition microarrays and a ratiometric design, in contrast to the cdc28 arrest described above, which used Affymetrix data. By focusing on each synchronization method individually, rather than using a merged dataset, we aimed to capture possible differences in the biology that might arise from different methods of synchronization, while also revealing the relationships that are robust across the three experiments and two assay platforms. For example, these data differ from each other in quality The ChIP/chip dataset is unique and was therefore used to build ANNs across cdc28, cdc15 and alpha factor experiments.

As demonstrated with the cdc28 data above we found these additional ANN models return the same core cell cycle regulators highlighted by the cdc28 ANNs. Six of these; Ndd1, Mbp1, Swi5, Stb1, Swi6, and Fkh2 are among the top seven regulators found, regardless of which cell cycle data and clusterings were used as input to the ANNs. This robustness in the central regulatory relationships is quite remarkable considering that, of 780 genes belonging to at least one of the cycling datasets, only 147 genes are common to all three experiments. Quantitation of pairwise clustering overlap, using the linear assignment metric, makes it very clear that the gene number and clustering patterns differ substantially (figure 7). Thus ANNs highlight major shared cell cycle relationships, even though the gene sets used and the clusterings are quite different. (table 1)

Cdc15ts-synchronized cells are arrested at the end of M phase (Spellman et al., 1998). Correspondingly, we find the expression cluster that peaks first – at 10 minutes in the Cdc15 data – associates

strongly with the early G1 factors Swi5 and Ace2 (EM1 in figure 7). Note that in the previous cdc28 ANN, the same association was made, even though – under that release condition – genes of this regulatory group are not upregulated until the second cycle after release ((Hart et al., 2005) and above). Alpha factor arrest is similar in this way to cdc28, reflecting their similar blockade points. Thus the ANNs easily related the cdc15 early G1 cluster to the alpha factor and cdc28 early G1 clusters, even though the cluster trajectory is strikingly different and the clusters themselves contain no individual genes in common with the cdc28 or alpha factor datasets (figures 5, 8, 9). Other high-ranking regulators appear in one or two, but not all three ANN cell cycle models. Yox1 and Yhp1, for example, differ among the models, because the gene classes derived from the RNA clusterings differ in content. Finally, Pho2 emerges as a potentially significant regulator associated with an M-phase kinetic pattern in the two Spellman datasets, consistent with the previously reported Pho2/Pho4 mediated, cell cycle expression for some phosphate regulated genes (Neef and Kladde, 2003). This is thought to be due to intracellular polyphosphate pools, which vary through the cycle in some culture conditions, but can also be influenced by growth media and history.

3 Discussion

We found that single layer artificial neural network (ANN) classifier models can effectively integrate global RNA expression and protein:DNA interaction data (ChIP/chip). The resulting models prominently highlight factors known to drive the transcriptional regulatory network underlying cell cycle phase specific expression. The weight matrices from these ANN models generally associated previously known cell cycle transcription factors with the cell cycle phase they are thought to regulate, and they did so as well as or better than other methods, based on flexible iterative thresholding (Bar-Joseph), network dynamics ((Luscombe et al., 2004)) or, most recently, Bayesian methods ((Sun et al.,

2006)). In general, we feel that more conventional statistical approaches and ANNs complement each other. Both generate hypothesized relationships and rank them. The strengths of the single layer neural network architecture used here is that it mirrors several basic properties of natural gene networks: 1) Both presence and absence of factor binding determine when and where a gene is expressed. 2) Factor occupancy *in vivo* is a continuum, not an all-or-nothing phenomenon, and the graded differences can have biological significance. For example, graded binding of the transcription factor Pha4 creates spatiotemporal gradients of target gene expression during pharyngeal development in *C. elegans* (Gaudet and Mango, 2002). These features of the neural network distinguish it from algorithms that depend solely on positive evidence of binding and require discretization of the binding signal to bound or unbound. A further distinction is that the neural network models can be easily and informatively "mutated" to ask how the overall network connection patterns and outputs are affected by specific changes, such as eliminating data for individual factors, combinations of factors, or making even larger structural changes. The obvious complementary strength of statistical methods is in quantitative thresholding based on significance measures.

A general conclusion that can be drawn from this work comes from the overall success of ANNs in classifying expression output according to transcription factor binding patterns. This might not have been true, but this overall observation argues strongly that transcriptional regulation, rather than differential post-transcriptional regulation, is the dominant mechanism in shaping phase specific RNA prevalence clusters. This observation does not preclude a role for other mechanisms operating on a minority of genes (perhaps explaining some difficult-to-predict genes) or a post-transcriptional role that is uniform over an entire class. For example, confusion matrix analysis of expression classes versus the predicted expression pattern from the ANNs identified a group of genes with EM3 (S phase) kinetics that comprise 10% of that cluster, but are associated with the EM2 G1 group by the ANN model (Figure

2), and these are reasonable candidates to be differentially regulated by post-transcriptional processes such as slower turnover.

3.1 Relating the Inferred Connections to Known Biology

The sum-of-squared weights metric proved to be simple and useful for objectively ranking regulators according to their importance in the network model, regardless of the input expression dataset. Even though ANN weights are not direct physical measures of binding, the resulting rankings correspond remarkably well with what is known from decades of work on transcription in the yeast cell cycle. The ANN models even highlighted subtle regulatory differences between different cell cycle synchronization methods. The top dozen of the 204 total regulators in the cdc28 ANN model contained 10 of 12 transcription factors present in the Harbison ChIP dataset and known to operate on cycling genes. Swi6 ranked at the top of the cell cycle regulators list in the cdc28, cdc15 and alpha factor ANN models and is always associated with G1 expression. Swi6 also shows a relative absence of binding to genes expressed highly during G2. The pattern of weights evaluated across the RNA expression clusters provide additional information. For instance, the cdc28 ANN weight vector for Mbp1 across the cell cycle clusters tracks very closely with Swi6 (Correlation coefficient r=.92). This mirrors underlying molecular biology in which Mbp1 and Swi6 combine to form the heteromeric active G1 transcription factor MBF. Stb1 is similarly grouped with Swi6 and Mbp1 as a co-regulator of G1 (cdc28 EM2) genes (r=.95 and .89 for Stb1 with Mbp1 or with Swi6, respectively). Ace2 and Swi5 are paralogous factors with similar DNA binding target sites (Dohrmann et al., 1996; Doolin et al., 2001), and both are positively associated with the early G1 (cdc28 EM 1) expression profile with similar in weights profiles (r= .71).

Also confirming expectations from studies of target genes and epistatsis predictions, Fkh1 and

Fkh2 were associated with cdc28 S/G2 expression clusters by the ANN. This inferred joint association is consistent with double knockout experiments, which indicate that the two complement each other (Zhu et al., 2000), and with studies showing the two factors bind the same sites in vitro (Hollenhorst et al., 2000). Examined in detail, the cdc28 ANN weights suggest a more nuanced view, in which both Fkh1 and Fkh2 are important for some genes in early S/G2 (EM3), whereas S/G2 class genes (cluster EM4) rely more heavily on NDD1 and Fkh2 and less on Fkh1. RNA expression data for Fkh1 and Fkh2 is consistent with this, since Fkh1 increases in expression nearly 20 minutes before Fkh2 in expression data collected by Cho et al., 1998. This is also consistent with a detailed study of *in vivo* binding at a few specific target genes (Hollenhurst et al., 2001), which showed that the two Fkh factors do not bind identically *in vivo*, and that there is a distinction between genes of the so-called Clb2 cluster (a subset of Cluster EM4 here), that are dominated by Fkh2 in conjunction with Mcm1/Ndd1, versus Fkh1 which is thought to bind independently. The alpha factor and cdc15 ANNs place diminished emphasis on Fkh1, compared with cdc28 ANNs, which is consistent with the idea that the two factors have different molecular activities and targets.

Time and sign of action. Cdc28 ANN Weight vectors for Mcm1 and Yox1 were also correlated (r=.69), defining an association with EM5 target genes where they displayed the two highest positive weights. They are known to act on some of the same genes, including EM5 group members (Pramila et al., 2002). In this example the ANN is picking up molecular effects that are of opposing molecular activity, with Yox1 repressing Mcm1 activity. This illustrates an issue of interpretation. Because the original binding data are from a mixed phase cell population, it reveals nothing about when during the cycle detected binding occurs. For positive acting factors whose binding and function are contemporaneous, we see a peak of binding simply correlated with a peak of RNA expression. But for a repressor acting on genes expressed in M phase, binding occurs at other times (late G1 , S, G2 alone, or in com-

binations (Pramila et al., 2002). Thus the ANN correctly connected the factor with its targets, but only by independently determining the mode of Yox1 action, or by adding temporally resolved binding data, can the sign and timing of action be discerned. For factors whose action - repressing or activating - is unknown or is conditional depending on context, temporally resolved ChIP data will be needed to infer the mode and time of action.

Swi4, a "missing" regulator. The ANN models did not assign high weight to Swi4, which one would expect to rank highly. Although Swi4 is a well known direct transcriptional regulator of Early G1 genes, providing the DNA binding moiety of SBF factor (Andrews and Herskowitz, 1989), it was not even close to the top 20 in the cdc28 aobANN, ranking 80 of 204. Its preferential association with G1 target genes only came to light when we performed in silico mutation analyses, eliminating one or more G1 factors. There are two possible explanations for its weak values in the wildtype ANNs, and they are not mutually exclusive. One simple possibility is that redundancy with other G1 regulatory factors is widespread, and this masks Swi4 when training the ANNs. Especially if coupled with generally less robust signals in the ChIP assay, the ANNs might have simply ignored Swi4. A second explanation is that Swi4 has greater breadth of binding across multiple clusters than its paralog, Mbp1. In this scenario, Swi4 spills over, binding to members of multiple cell cycle expression clusters when compared with other G1-specific regulators such as Mbp1, Swi6, or Stb1. This would give Swi4 less discrimination power in classifying genes, despite active G1 binding and could arise from purely technical issues, or from an unappreciated biological role outside its function in SBF.

An independent analysis of the Harbison ChIP data in the context of a much larger library of expression data across many conditions other than cell cycle phases, using a different computational approach, supports the idea of broad Swi4 distribution among cell cycle regulatory classes (Bar-Joseph et al., 2003). Specifically, the GRAM algorithm uses co-expression patterns to incorporate into the con-

nection map ChIP interactions that are below statistical significance when evaluated on their own (Lee et al., 2002; Bar-Joseph et al., 2003; Harbison et al., 2004). They reported regulatory modules consisting of pairs of factors in which Swi4 is partnered by binding and expression data with one or more factors from each and every expression cluster: Ace2, Fhk2, Ndd1 and Mcm1, as well as the "classic" associated G1 factors, Mbp1, Stb1, Swi6. In addition, an entirely independent set of ChIP/chip measurements and analysis from Snyder and colleagues (Horak et al., 2002) showed substantial Swi4 binding activity upstream of non-G1 genes. Taken together, these data suggest Swi4 might have one or more previously unappreciated functions within exponentially growing cells that are distinct from its classic role as part of SBF.

Finally, a picture of partly, but not entirely, redundant functions for the Swi4/Mbp1 paralogs was also emphasized in a recent genetic study (Bean et al., 2005). We therefore think it likely that the way the unperturbed ANNs treat Swi4 reflects partial biological redundancy combined with its more widely distributed binding across non-G1 clusters.

3.2 Potential Newly Identified Regulatory Connections

Do the ANNs suggest new factors associated phase specific expression? Focusing on the cdc28 example, and using stability across ANNs as an added filtering criterion, factors ranking above Leu3 stood out. In particular, both Usv1 and Dal81 are interdigitated among the otherwise well-documented ten major regulators cell cycle regulators, although not previously associated with this function to our knowledge. A different explanation is that factors like Usv1, Dal81, and a handful of others ranking in the top 20, may be in the ANN model for reasons having nothing to do with the cell cycle explicitly, but having much to do with the partially overlapping architecture of transcriptional networks in eukaryotes. Thus, we expect that some genes – perhaps most – within cycling clusters will also belong to one or

more other functional modules. In the context of those other functions, they will presumably be regulated by factors that have nothing to do with directing cell cycle phase patterns. This kind of network intersection and partial overlap is strikingly evident in global module maps (Segal et al., 2003a). Some factors appearing in the ANN top 20 may be there for this reason. There are others (Pho2, for example) that seem to be drawn into regulating phase specific expression because of metabolic links (in this case through polyphosphate pools and membrane biogenesis ((Neef and Kladde, 2003)). We expect that the overall approach we have taken for the cell cycle network, using global ChIP/chip data, could easily be extended to any network whose states of interest are well represented in available ChIP/chip data, and whose RNA datasets are of sufficient quality and resolution to cluster the expression behaviors of interest. However, a decisive improvement in sophistication of the ANN model, and the hypotheses it generates, will come with time-resolved ChIP data.

3.3 Neural network weights predict evolutionarily conserved binding motif frequencies

If binding data are predictive of expression class, and if meaningful transcription factor binding is motif specific, then it should be possible to independently verify relationships from the weights matrix by measuring the frequency of binding motifs. We can also ask if any observed site enrichment and depletion are evolutionarily conserved, as would be expected if they mediate functionally relevant factor binding. Motif frequency across cell cycle clusters in multiple yeast species correlated remarkably well with binding probabilities from the ChIP data and also with the ANN weights trajectories across the same clusters (Figure 10). The conserved motif data for Mbp1 and Swi5/Ace2, and Fkh1/Fkh2, all factors with well-defined binding motifs, provided independent support for conclusions from the ANN, since the ANN was constructed without any input information about DNA sites.

3.4 Conservation of site enrichment and depletion over great evolutionary distance

The distribution of MCB sites across the cycle phases was striking and prompted us to ask if both enrichment and depletion holds over very great evolutionary distance. If specific depletion is a functionally important network characteristic, then we would predict that it would retained over very great evolutionary distance. We performed the same site enrichment analysis across cell cycle gene classes in *S. pombe*, which is said to be as distant from budding yeast as are humans (~ 500my). We used the EM algorithm to cluster the *S. pombe* cycling data of (Rustici et al., 2004) in the same way that the various Sacharomyces experiments had been clustered (Hart et al., 2005). At this evolutionary distance there are no large blocks of conserved noncoding DNA sequence. *S. pombe* does, however, have an identified MBF ortholog, and the short binding motif for MBF shows significant site enrichment in our expression cluster 3, together with significant depletion from cluster 5, mirroring the pattern in budding yeast (figure 11). The positive regulator-to-target group conservation was noted previously (Rustici et al., 2004; Peng et al., 2004; Oliva et al., 2005), but in this study we were able to detect it without strongly pre-filtering gene sets for their explicit experimental responsiveness to MBF. The new observation here is that depletion of MBF sites, operating specifically in the group of genes normally expressed later in the cell cycle, is a very highly-conserved property. This cis-motif depletion suggests there is selective restriction against MBF sites and that it is phase specific: it does not apply broadly to most genes in the genome, but does apply preferentially to genes in late cell cycle cluster (in this case cluster 5 for S. pombe, cluster 4 for *S. cerevisae*). In both organisms, this cluster contains genes whose products are involved in mitosis, and it seems possible that their heterochronic expression during G1/S phases, as MCB sites might cause, could disrupt proper control or execution of S phase. However, the observed conservation is apparently a network property, even though the specific genes

in each phase group are – mainly – not orthologous. Thus the surprising observation that most genes in these oscillating clusters are not the same ones in pombe and Saccharomyces (reviewed in (Bahler, 2005)), if correct, suggests that conserved enrichment and depletion of regulatory motifs are network architecture properties that are shared across hundreds of millions of years, even though most specific genes involved are different.

4 Methods

4.1 Data Pre-processing

The primary expression dataset for modeling is Affymetrix microarray data measuring RNA levels of nearly every gene in yeast through two cell cycles, following release from conditional CDC28TS arrest (Cho et al., 1998). That time course sampled RNA levels at 10 minute intervals over 170 minutes, which covers two cycles. These data were obtained from the original authors and preprocessed in three steps. 1) Any gene that did not show sustained absolute expression greater than the 2.5% quantile of the data (an absolute signal of 8) for three consecutive timepoints was eliminated. 2) For the remaining 6174 expression vectors, each time point measurement was divided by the median expression value across all time points for the gene. 3) The log2 of each ratio was then taken and these values comprised the expression matrix for all further analysis. For key model building in this work, we focused on the subset of expression vectors (384) that had been identified by Cho et. al. as displaying a cell cycle dependent pattern and also passed the above filter for absolute expression, operationally we refer to this set as the "cycling" set.

The primary *in vivo* protein:DNA interaction dataset (ChIP/array) used here is from Harbison et al. (2004). These data were obtained at http://web.wi.mit.edu/young/regulatory_code/ and the re-

ported P-values were used directly. Briefly, for each of 204 transcriptional regulators, Harbison and colleagues constructed a yeast strain containing a myc-epitope-tagged version of the factor that was inserted into the corresponding transcription factor locus. Each strain was used to perform three independent ChIP/array measurements taken from freely cycling exponential phase cultures. The cells were subjected to standard formaldehyde crosslinking to attach transcription factors to their *in vivo* binding sites, the chromatin was sheared, factor bound DNA was enriched by IP, amplified by LMPCR and fluorescently labeled. ChIP enriched DNA was then co-hybridized with control DNA to microarrays containing essentially all intergenic sequences in yeast. A binding ratio was then calculated for each array feature based on the relative hybridization signal for targets synthesized from ChIP enriched DNA vs. whole cell extract control DNA . Three biological replicate experiments were performed, each beginning from an independent yeast culture. Based on an error model first described in (Hughes et al., 2000) and the three replicate binding ratios for each intergenic sequence, a P-value was reported for each upstream intergenic sequence. This p-value roughly estimates the probability that a given transcription factor is bound to a particular intergenic sequence.

4.2 Neural Network Implementation and Training

Figure 1 illustrates the overall structure of the artificial neural networks (ANN) trained in this study. Backpropagation was implemented by the UWBP package (Maclin et al., 1992) to train a single layer network with no hidden units. Each ANN was trained using 300 epochs using a learning rate of .002. RNA expression array data for the subset of 384 cycling genes as described above were clustered using an expectation maximization algorithm fitting the data to a mixture of Gaussians probability distributions with a diagonal covariances (EM MoDG (Hart et al., 2005; Dempster et al., 1977). Networks to predict cluster membership for each gene based on an input vector composed of ChIP derived in-

vivo factor binding probabilities for the 204 measured regulators in the Harbison dataset. Individual networks were trained using 80% of the data and tested on 20% of the data. For each 80/20 dataset split, ten neural networks were trained using different random seeds for each network. The network with the best prediction accuracy on the testing dataset was then selected and denoted as “best”. This process was then repeated 40 times splitting the dataset into different testing and training datasets. The network weights from the resulting 40 selected “best” networks were then averaged together to create the average-of-bests neural network (aobANN). We focus on this network for subsequent biological interpretation, with the primary goal of identifying regulatory connections between transcription factors and their direct target genes. Because the purpose of this network is not to repeatedly classify similar data, the implications of overtraining are different than they would be for classical uses of ANNs. In this unconventional usage we show by measuring the behavior of 10 internal "gold standard" known cell cycle regulators, that any "overtraining" is not deleterious for the intended goal, which is extracting a series of ranked hypotheses about regulator-to-output relationships. Regulators within aobANNs are ranked based on the median sum-of-squares rank across all of the individual ANNs trained to generate the aobANN. The sum-of-squares ranking for a regulator within an individual network is simply the sum of squared weights across the classes in the weight matrix ($\sum_c w_{c,r}^2$).

4.2.1 Consensus Site Enrichment and Depletion Calculations:

In order to determine whether an expression cluster showed an enrichment in genes that contain a particular consensus site we calculated the likelihood of the observed enrichment, or depletion, being a chance occurrence according to a binomial model of occurrence probabilities. We count the observed number of genes that have at least one instance of a consensus sequence within the 1KB directly upstream of the coding sequence for all genes in an expression cluster versus the number of genes that would be expected by chance. As no known background sequence model is completely provably

correct, for each consensus sequence we calculate the expected background frequency ($\hat{f}$) using a bootstrapping method. We randomly selected 1000 different sets of genes the same size as the cluster being compared (n). These randomly selected background sets are drawn from either the entire genome or from only the "cycling" genes, which were used in training the ANNs. The number of genes that contain at least a single instance of the consensus is counted for each randomly selected set. The average count across the 1000 samples is normalized and used as our estimate of the expected number of genes within a cluster that have a single occurrence within 1KB upstream (E_c). Since the chances of any given gene within a cluster having a given consensus sequence within the 1KB upstream can be assumed to be independent, we can estimate the probability of finding the observed number of counts (O_c) using a standard binomial distribution (1). If the site is enriched we estimate the p-value for the likelihood of finding at least the observed count, but if the site is depleted we calculate likelihood of finding at most the observed count (equation 2).

$$P(i|c,n) = \binom{n}{i} \left(\frac{c}{n}\right)^i \left(1 - \frac{c}{n}\right)^{n-i} \tag{1}$$

$$p = \begin{cases} \sum_{i=0_c}^{n} P(i|E_c,n) & \text{if } O_c > E_c \\ 1 - \sum_{i=0_c}^{n} P(i|E_c,n) & \text{if } O_c \leq E_c \end{cases} \tag{2}$$

References

Andrews, B. and Herskowitz, I. (1989). The yeast swi4 protein contains a motif present in developmental regulators and is part of a complex involved in cell-cycle-dependent transcription. *Nature*, 342:830–3.

Bahler, J. (2005). Cell-cycle control of gene expression in budding and fission yeast. *Annu Rev Genet*,

39:69–94.

Bar-Joseph, Z., Gerber, G. K., Lee, T. I., Rinaldi, N. J., Yoo, J. Y., Robert, F., Gordon, D. B., Fraenkel, E., Jaakkola, T. S., Young, R. A., and Gifford, D. K. (2003). Computational discovery of gene modules and regulatory networks. *Nat Biotechnol*, 21:1337–42.

Bean, J. M., Siggia, E. D., and Cross, F. R. (2005). High functional overlap between mlui cell-cycle box binding factor and swi4/6 cell-cycle box binding factor in the g1/s transcriptional program in saccharomyces cerevisiae. *Genetics*, 171:49–61.

Bishop, C. (1995). *Neural Networks for Pattern Recognition*. Oxford University Press.

Breeden, L. L. (2000). Cyclin transcription: Timing is everything. *Curr Biol*, 10:R586–8.

Breeden, L. L. (2003). Periodic transcription: A cycle within a cycle. *Curr Biol*, 13(1):R31–8.

Cho, R. J., Campbell, M. J., Winzeler, E. A., Steinmetz, L., Conway, A., Wodicka, L., Wolfsberg, T. G., Gabrielian, A. E., Landsman, D., Lockhart, D. J., and Davis, R. W. (1998). A genome-wide transcriptional analysis of the mitotic cell cycle. *Mol Cell*, 2(1):65–73.

Cho, R. J., Huang, M., Campbell, M. J., Dong, H., Steinmetz, L., Sapinoso, L., Hampton, G., Elledge, S. J., Davis, R. W., and Lockhart, D. J. (2001). Transcriptional regulation and function during the human cell cycle. *Nat Genet*, 27(1):48–54.

Costanzo, M., Schub, O., and Andrews, B. (2003). G1 transcription factors are differentially regulated in saccharomyces cerevisiae by the swi6-binding protein stb1. *Mol Cell Biol*, 23:5064–77.

de Lichtenberg, U., Wernersson, R., Jensen, T. S., Nielsen, H. B., Fausboll, A., Schmidt, P., Hansen, F. B., Knudsen, S., and Brunak, S. (2005). New weakly expressed cell cycle-regulated genes in yeast. *Yeast*, 22(15):1191–1201.

Dempster, A., Laird, N., and Rubin, D. (1977). Maximum lielihood from incomplete data via the em algorithm. *J. Royal Statistical Society, Series B*, 39:1–38.

Dohrmann, P. R., Voth, W. P., and Stillman, D. J. (1996). Role of negative regulation in promoter specificity of the homologous transcriptional activators ace2p and swi5p. *Mol Cell Biol*, 16:1746–58.

Doolin, M., Johnson, A., Johnston, L., and Butler, G. (2001). Overlapping and distinct roles of the duplicated yeast transcription factors ace2p and swi5p. *Mol Microbiol*, 40:422–32.

Gao, F., Foat, B. C., and Bussemaker, H. J. (2004). Defining transcriptional networks through integrative modeling of mrna expression and transcription factor binding data. *BMC Bioinformatics*, 5:31.

Gaudet, J. and Mango, S. E. (2002). Regulation of organogenesis by the caenorhabditis elegans foxa protein pha-4. *Science*, 295:821–5.

Harbison, C. T., Gordon, D. B., Lee, T. I., Rinaldi, N. J., Macisaac, K. D., Danford, T. W., Hannett, N. M., Tagne, J. B., Reynolds, D. B., Yoo, J., Jennings, E. G., Zeitlinger, J., Pokholok, D. K., Kellis, M., Rolfe, P. A., Takusagawa, K. T., Lander, E. S., Gifford, D. K., Fraenkel, E., and Young, R. A. (2004). Transcriptional regulatory code of a eukaryotic genome. *Nature*, 431:99–104.

Hart, C. E., Sharenbroich, L., Bornstein, B. J., Trout, D., King, B., Mjolsness, E., and Wold, B. J. (2005). A mathematical and computational framework for quantitative comparison and integration of large-scale gene expression data. *Nucleic Acids Res*, 33:2580–94.

Hollenhorst, P. C., Bose, M. E., Mielke, M. R., Muller, U., and Fox, C. A. (2000). Forkhead genes in transcriptional silencing, cell morphology and the cell cycle. overlapping and distinct functions for fkh1 and fkh2 in saccharomyces cerevisiae. *Genetics*, 154:1533–48.

Horak, C. E., Luscombe, N. M., Qian, J., Bertone, P., Piccirrillo, S., Gerstein, M., and Snyder, M. (2002). Complex transcriptional circuitry at the g1/s transition in saccharomyces cerevisiae. *Genes Dev*, 16(23):3017–33.

Hughes, T. R., Marton, M. J., Jones, A. R., Roberts, C. J., Stoughton, R., Armour, C. D., Bennett, H. A., Coffey, E., Dai, H., He, Y. D., Kidd, M. J., King, A. M., Meyer, M. R., Slade, D., Lum, P. Y., Stepaniants, S. B., Shoemaker, D. D., Gachotte, D., Chakraburtty, K., Simon, J., Bard, M., and Friend, S. H. (2000). Functional discovery via a compendium of expression profiles. *Cell*, 102(1):109–26.

Iyer, V., Horak, C., Scafe, C., Botstein, D., Snyder, M., and Brown, P. (2001). Genomic binding sites of the yeast cell-cycle transcription factors sbf and mbf. *Nature*, 409:533–8.

Koch, C., Moll, T., Neuberg, M., Ahorn, H., and Nasmyth, K. (1993). A role for the transcription factors mbp1 and swi4 in progression from g1 to s phase. *Science*, 261:1551–7.

Koranda, M., Schleiffer, A., Endler, L., and Ammerer, G. (2000). Forkhead-like transcription factors recruit ndd1 to the chromatin of g2/m-specific promoters. *Nature*, 406:94–8.

Lee, I., Date, S. V., Adai, A. T., and Marcotte, E. M. (2004). A probabilistic functional network of yeast genes. *Science*, 306(5701):1555–1558.

Lee, T. I., Rinaldi, N. J., Robert, F., Odom, D. T., Bar-Joseph, Z., Gerber, G. K., Hannett, N. M., Harbison, C. T., Thompson, C. M., Simon, I., Zeitlinger, J., Jennings, E. G., Murray, H. L., Gordon, D. B., Ren, B., Wyrick, J. J., Tagne, J. B., Volkert, T. L., Fraenkel, E., Gifford, D. K., and Young, R. A. (2002). Transcriptional regulatory networks in saccharomyces cerevisiae. *Science*, 298(5594):799–804.

Luscombe, N. M., M, M. B., a. b. u. Madan, B., Yu, H., Snyder, M., Teichmann, S. A., and Gerstein,

M. (2004). Genomic analysis of regulatory network dynamics reveals large topological changes. *Nature*, 431:308–12.

M. A. Beer, S. T. (2004). Predicting gene expression from sequence. *Cell*, 117:185–98.

Maclin, R., Opitz, D., and Shavlik, J. W. (1992). University of wisconsin-madison backpropagation (uwbp).

Menges, M., Hennig, L., Gruissem, W., and Murray, J. A. (2003). Genome-wide gene expression in an arabidopsis cell suspension. *Plant Mol Biol*, 53:423–42.

Mjolsness, E., Sharp, D. H., and Reinitz, J. (1991). A connectionist model of development. *J Theor Biol*, 152(4):429–53.

Neef, D. W. and Kladde, M. P. (2003). Polyphosphate loss promotes snf/swi- and gcn5-dependent mitotic induction of pho5. *Mol Cell Biol*, 23(11):3788–3797.

Oliva, A., Rosebrock, A., Ferrezuelo, F., Pyne, S., Chen, H., Skiena, S., Futcher, B., and Leatherwood, J. (2005). The cell cycle-regulated genes of schizosaccharomyces pombe. *PLoS Biol*, 3:e225.

Peng, X., Karuturi, R. K., Miller, L. D., Lin, K., Jia, Y., Kondu, P., Wang, L., Wong, L. S., Liu, E. T., Balasubramanian, M. K., and Liu, J. (2004). Identification of cell cycle-regulated genes in fission yeast. *Mol Biol Cell*.

Pramila, T., Miles, S., GuhaThakurta, D., Jemiolo, D., and Breeden, L. L. (2002). Conserved homeodomain proteins interact with mads box protein mcm1 to restrict ecb-dependent transcription to the m/g1 phase of the cell cycle. *Genes Dev*, 16:3034–45.

Reinitz, J., Mjolsness, E., and Sharp, D. H. (1995). Model for cooperative control of positional information in drosophila by bicoid and maternal hunchback. *J Exp Zool*, 271(1):47–56.

Rustici, G., Mata, J., Kivinen, K., Lio, P., Penkett, C. J., Burns, G., Hayles, J., Brazma, A., Nurse,

P., and Bahler, J. (2004). Periodic gene expression program of the fission yeast cell cycle. *Nat Genet*, 8:809–817.

Segal, E., Shapira, M., Regev, A., Pe'er, D., Botstein, D., Koller, D., and Friedman, N. (2003a). Module networks: identifying regulatory modules and their condition-specific regulators from gene expression data. *Nat Genet*, 34:166–76.

Segal, E., Yelensky, R., and Koller, D. (2003b). Genome-wide discovery of transcriptional modules from dna sequence and gene expression. *Bioinformatics*, 19 Suppl 1:i273–i282.

Spellman, P. T., Sherlock, G., Zhang, M. Q., Iyer, V. R., Anders, K., Eisen, M. B., Brown, P. O., Botstein, D., and Futcher, B. (1998). Comprehensive identification of cell cycle-regulated genes of the yeast saccharomyces cerevisiae by microarray hybridization. *Mol Biol Cell*, 9(12):3273–97.

Sun, N., Carroll, R. J., and Zhao, H. (2006). Bayesian error analysis model for reconstructing transcriptional regulatory networks. *Proc Natl Acad Sci U S A*, 103(21):7988–7993.

Tsai, H. K., Lu, H. H., and Li, W. H. (2005). Statistical methods for identifying yeast cell cycle transcription factors. *Proc Natl Acad Sci U S A*, 102:13532–7.

Vohradsky, J. (2001). Neural model of genetic network. *J Biol Chem*, 276(39):36168–36173.

Wang, W., Cherry, J. M., Botstein, D., and Li, H. (2002). A systematic approach to reconstructing transcription networks in saccharomyces cerevisiae. *Proc Natl Acad Sci U S A*, 99(26):16893–16898.

Weaver, D. C., Workman, C. T., and Stormo, G. D. (1999). Modeling regulatory networks with weight matrices. *Pac Symp Biocomput*, pages 112–23.

Whitfield, M. L., Sherlock, G., Saldanha, A. J., Murray, J. I., Ball, C. A., Alexander, K. E., Matese,

J. C., Perou, C. M., Hurt, M. M., Brown, P. O., and Botstein, D. (2002). Identification of genes periodically expressed in the human cell cycle and their expression in tumors. *Mol Biol Cell*, 13(6):1977–2000.

Workman, C. T., Mak, H. C., McCuine, S., Tagne, J. B., Agarwal, M., Ozier, O., Begley, T. J., Samson, L. D., and Ideker, T. (2006). A systems approach to mapping dna damage response pathways. *Science*, 312(5776):1054–1059.

Zhang, M. Q. (1999). Large-scale gene expression data analysis: a new challenge to computational biologists [published erratum appears in genome res 1999 nov;9(11):1156]. *Genome Res*, 9(8):681–8.

Zhu, G., Spellman, P. T., Volpe, T., Brown, P. O., Botstein, D., Davis, T. N., and Futcher, B. (2000). Two yeast forkhead genes regulate the cell cycle and pseudohyphal growth. *Nature*, 406:90–4.

5 Figures and Tables

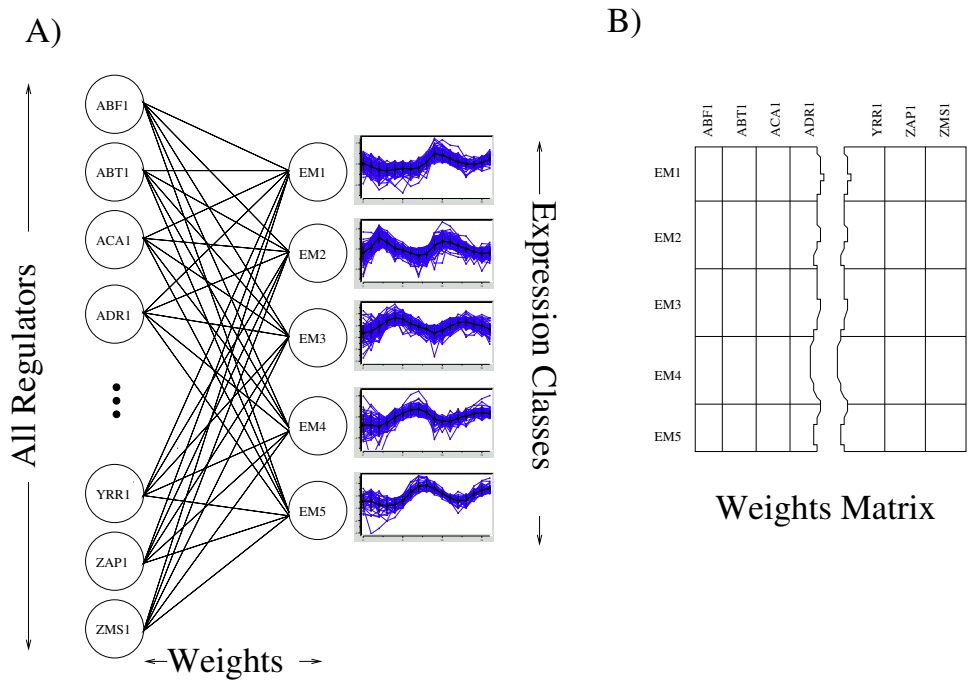

Figure 1: **The Artificial Neural Network Architecture (ANN)** A) Shown is the simple single layer network we trained to predict expression behavior based on the *in vivo* binding activity of $\sim 75\%$ of the transcription regulators in yeast. A 204 dimension vector containing the measured binding data from (Harbison et al., 2004) is used as the input vector. Given this binding vector the ANN was trained to predict during which of the five canonical cell cycle expression groups it is likely to be expressed. These expression classes were determined using EM MoDG. B) Matrix representation of the ANN. Each matrix cell, $W_{c,r}$, represents the real-valued connection strength, or weight, between a regulator (r) and an expression class (c) and is shown in A as an edge between a regulator and an expression class. These weights represent the importance of a regulator's binding activity or inactivity in the associated expression class

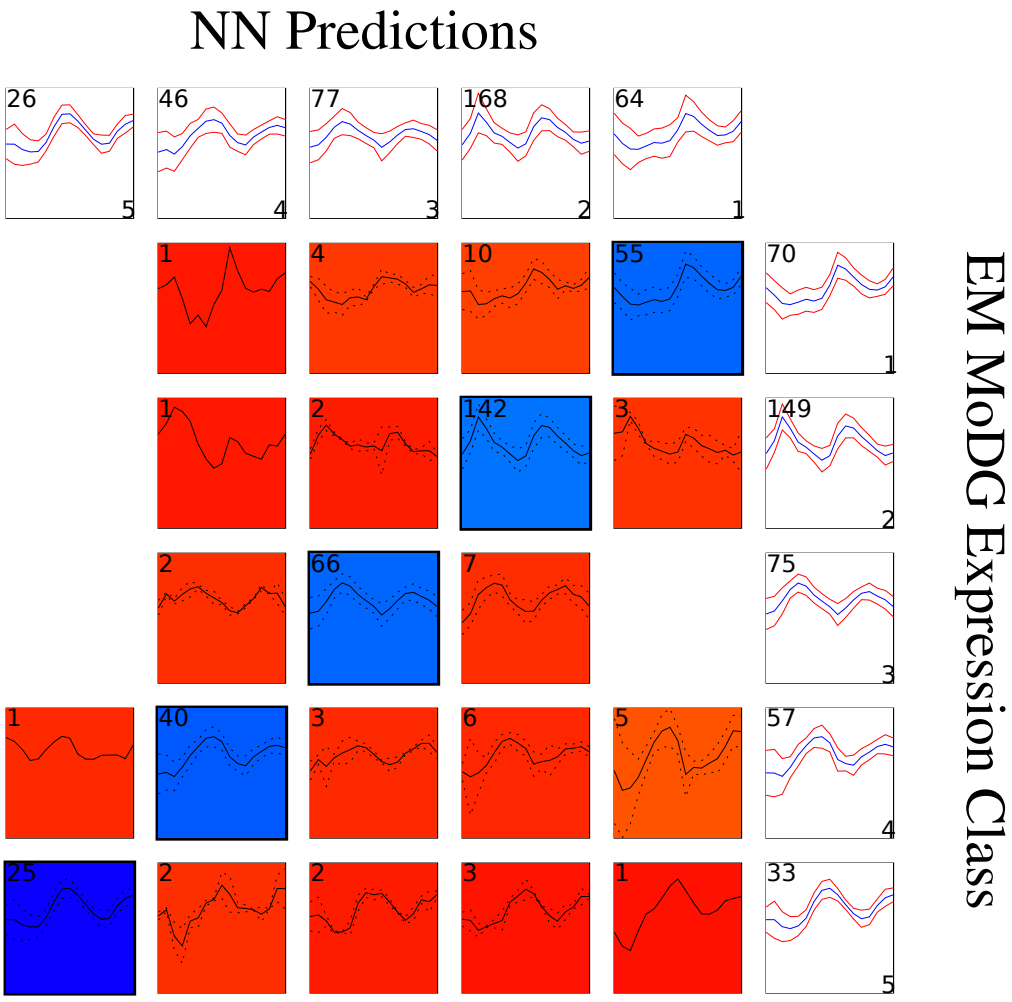

Figure 2: **Confusion Array showing the average-of-best ANN vs EM MoDG expression classes**. Here we compare the expression class prediction of the average-of-bests ANN which was created by averaging 40 ANNs trained to predict expression behavior from the binding data available for a gene. Each of the 40 ANNs were trained on 80% of the data and tested on the remaining 20% and they were selected as the best performing network out 10 networks trained on the same data split but initialized with differing seeds. These two classifications have a similarity of .86 by linear assignment (Hart et al., 2005)

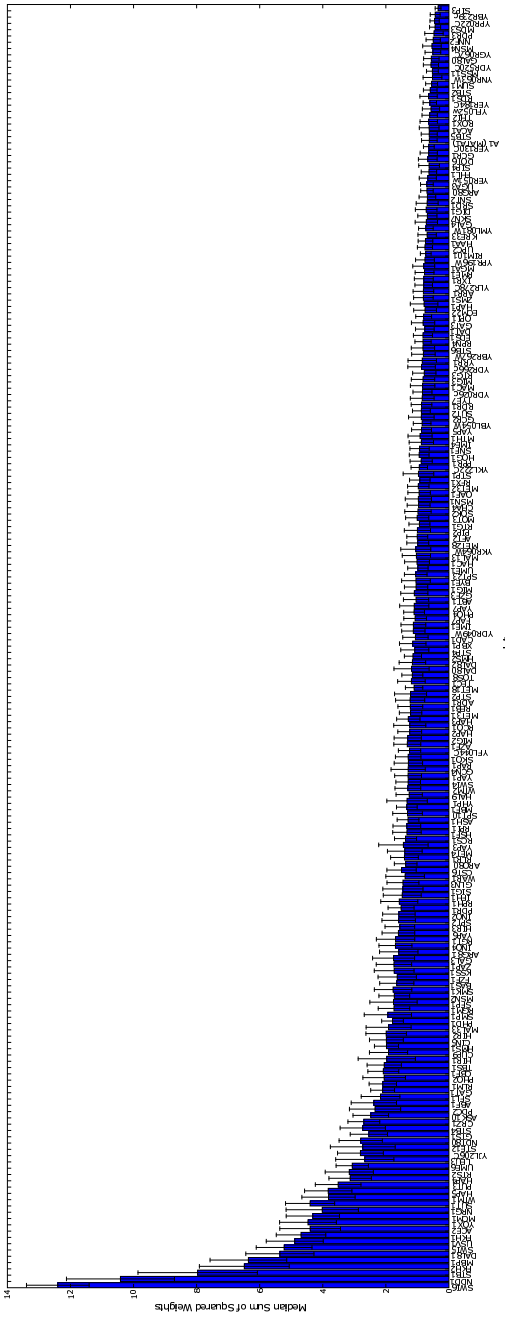

(a) Sum of Squared Weights Distribution

Figure 3

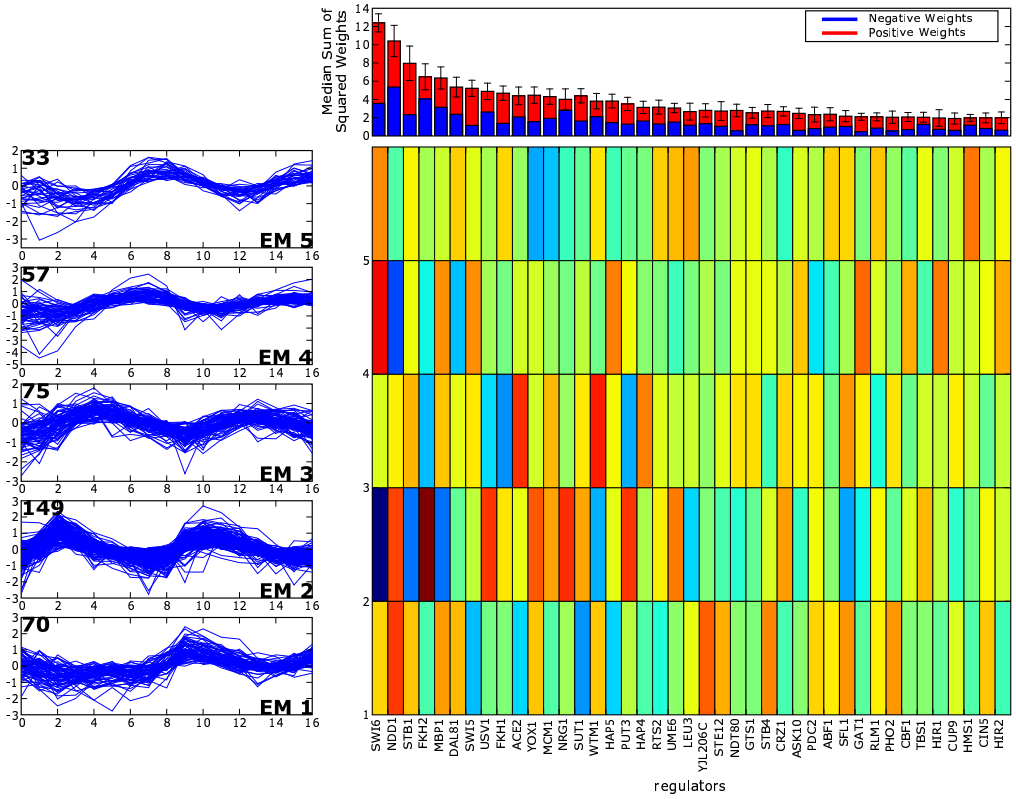

(b) Details of top Regulators

Figure 3

Figure 3: **Weight matrix for the Average-of-bests ANN**. a) Regulators were sorted based on the sum-of-squares metric (methods), and the total sum-of-square rank is plotted as a bar for each regulator. b) Shown are the top 20 regulators after sorting each regulator by importance in predicting expression behavior using a sum-of-squared weights measure. The top panel reproduces a zoomed in view of the top 20 regulators as in panel a. Here each regulator's bar is split into positive weights (red) and negative weights (blue). The left hand column shows a trajectory summary for each expression cluster as classified by EM MoDG. The right hand color map represents the weight matrix where expression classes are displayed along the rows corresponding to the drawn trajectory summaries. Regulators are sorted along the columns in rank order. Each cell is colored proportional to its value in the weight matrix.

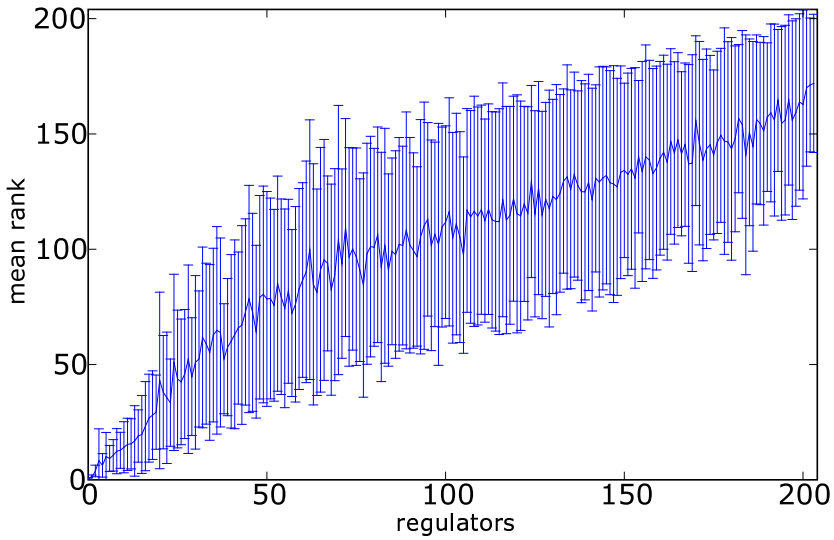

(a) All Regulators

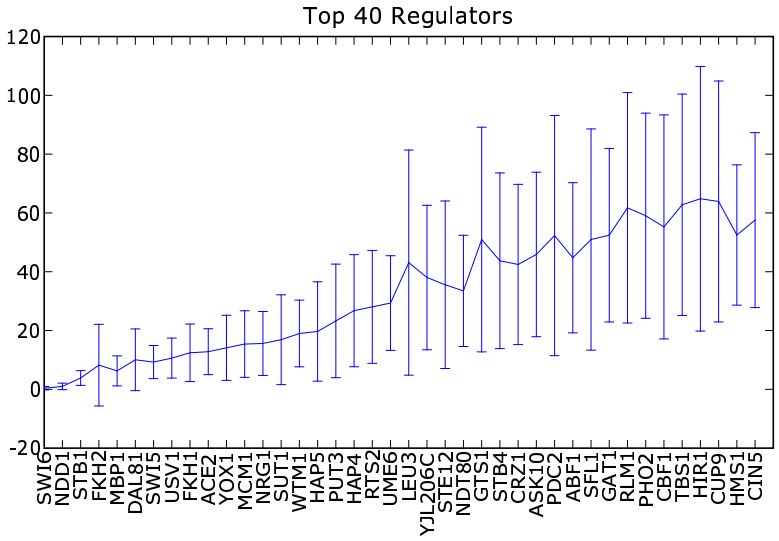

(b) Top 40 Regulators

Figure 4: **Neural Network Rank Order Stability** a) Shown are the regulators sorted by their sum-of-squares rank order (see methods). The line shows the mean ranking for each regulator across each of the 40 selected best ANNs, with the variance of each ranking shown as errorbars. b) shows the top 20 regulators which show quite high stability.

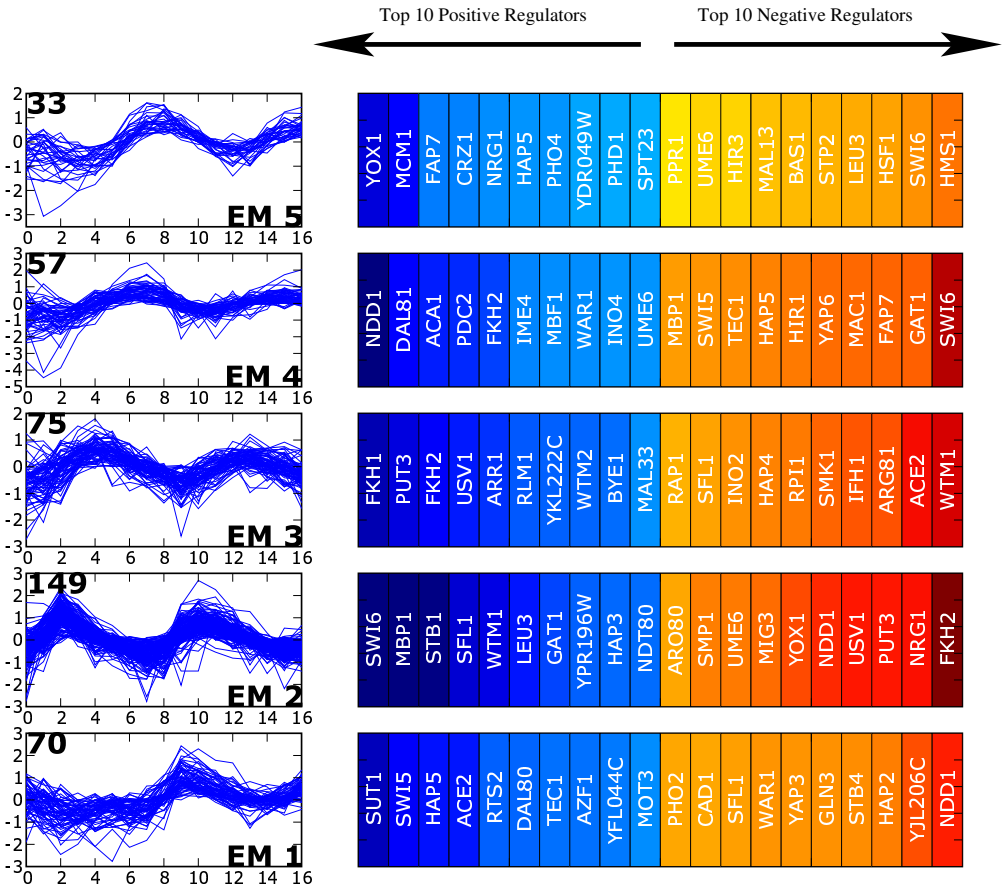

Figure 5: **ANN weights sorted on an expression class basis**. Shown are the ANN weights from the average-of-best network as in figure 3 with the exception that the top and bottom regulators for each class are displayed. The regulator ranking for each class is simply based on its weight in the weight matrix for each expression class. Detailed annotations for these regulators are listed in table 1

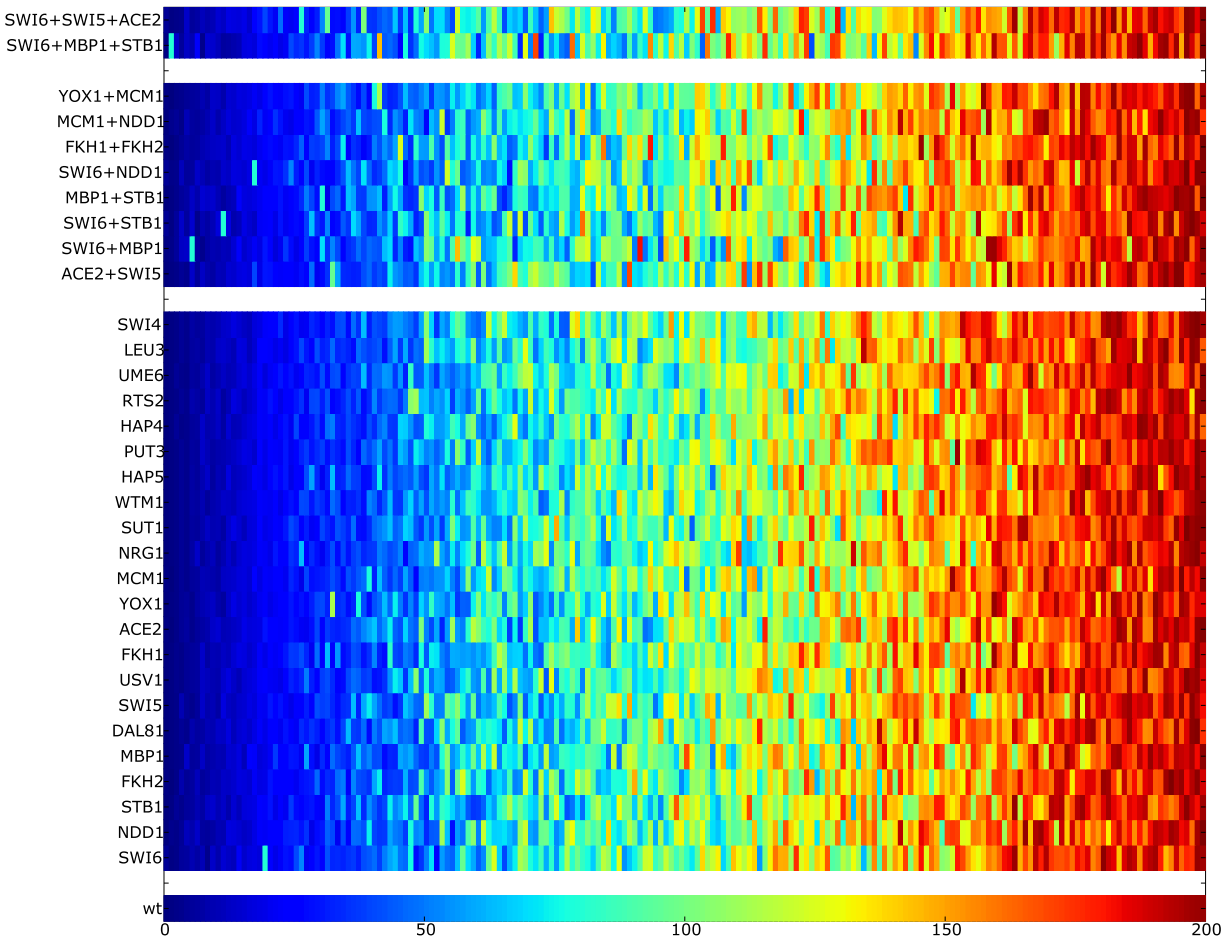

(a) Overview of network changes

Figure 6

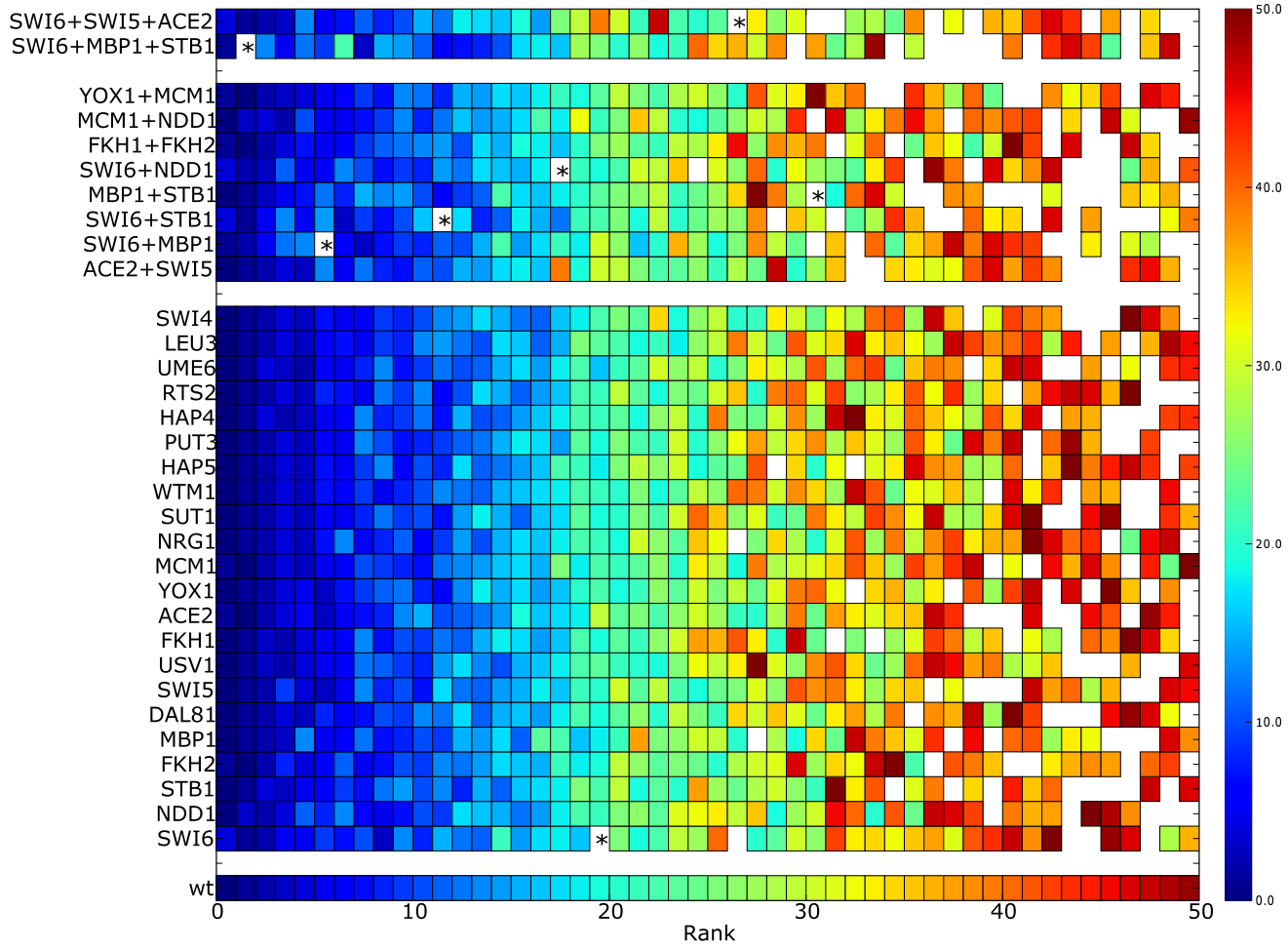

(b) Network changes for the top 50 regulators

Figure 6

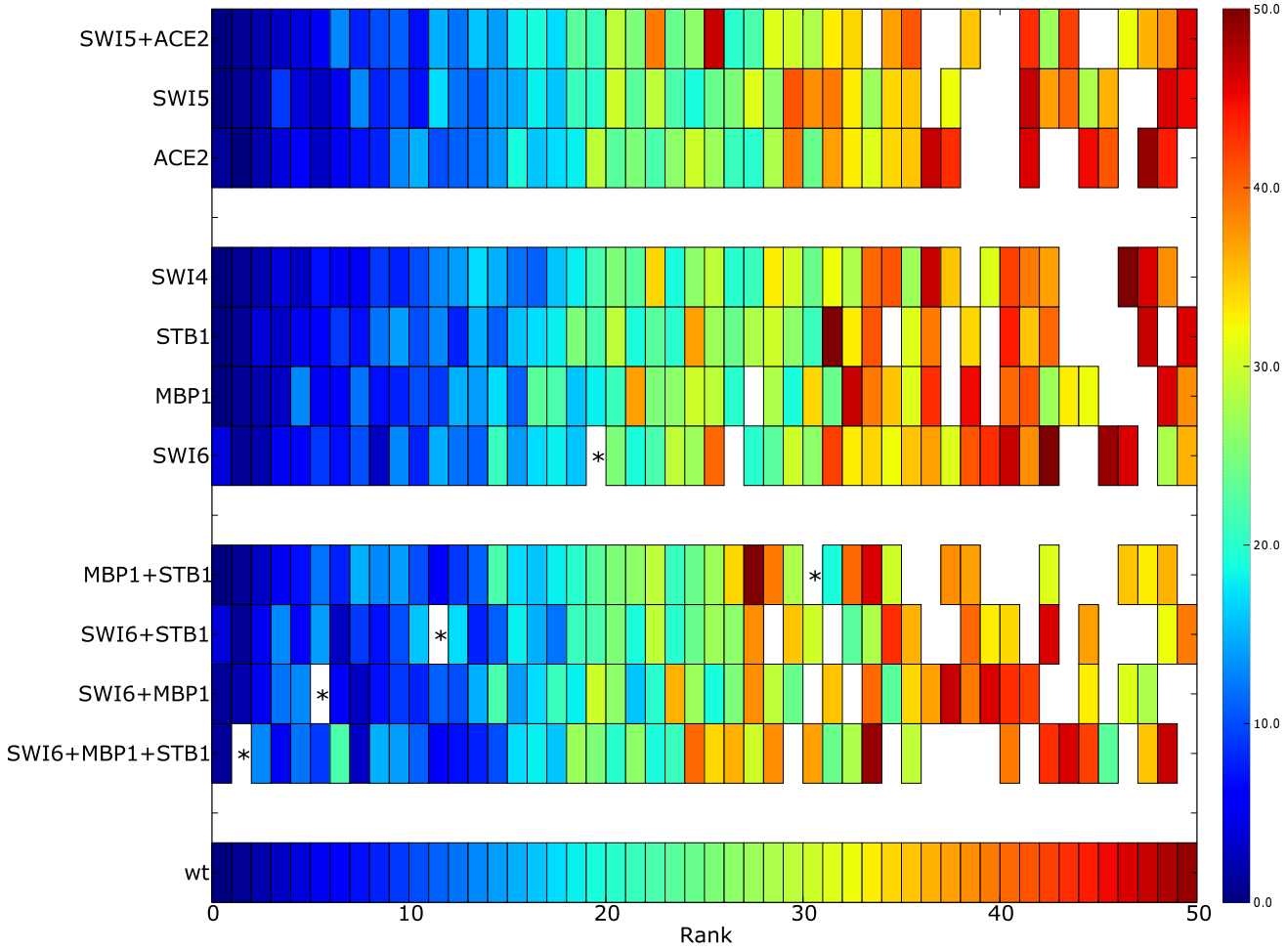

(c) Highlights of G1 network changes

Figure 6

Figure 6: *in silico* **network mutations** Shown are results from training ANNs missing one or more regulators as indicated on the left margin of each heatmap. Within each heatmap each cell represents a regulator, the position of the cell along the x-axis of the plot is determined by the mutated network, but the color is indicative of the regulator's rank in the unperturbed network (as shown in figure 3). The lowest strip shows the rank order color spectrum for the wildtype network a) An overview showing the overall rank stability of the regulators across all mutant networks generated. b) A higher resolution view of the top ranked regulators for each mutant network. Only the top 50 regulators are shown, and the color spectrum is adjusted to only span 1-50. Any regulator that was ranked within the top 50 regulators in a mutant network, but not in the wildtype network is shown as white. The position of Swi4 in each network is denoted by '*'. c) A zoomed in version of our mutant network analysis focusing only on networks generated by the top G1 regulators (Swi6, Mbp1, Stb1, Ace2, Swi5, Swi4).

	Synchronization Method		
	Alpha Factor	Cdc15	Cdc28
Alpha Factor	1.00	0.57	0.61
Cdc15	-	1.00	0.47
Cdc28	-	-	1.00

Table 1: Similarity of clustering results from different synchronization methods as measured by Linear Assignment (Hart et al., 2005).

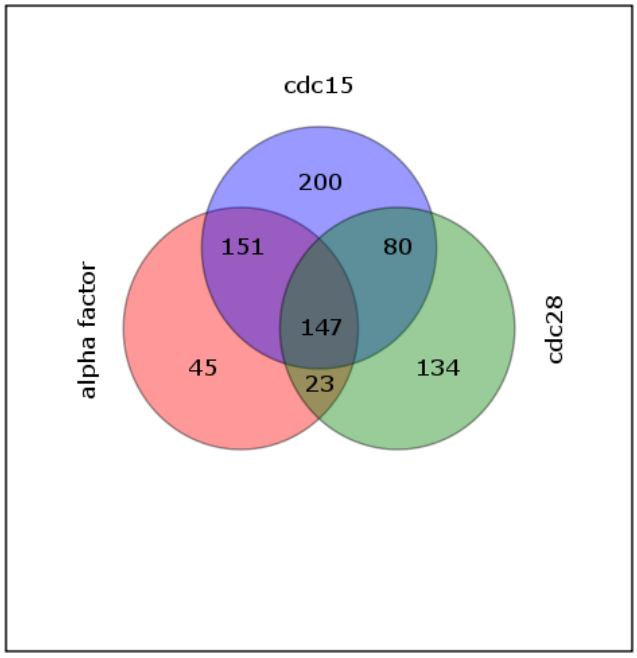

Figure 7: **Overlap of cell cycle groups**. Venn Diagram illustrating the total number of genes that are cycling in each of the three synchronization methods after our filtering and normalization.

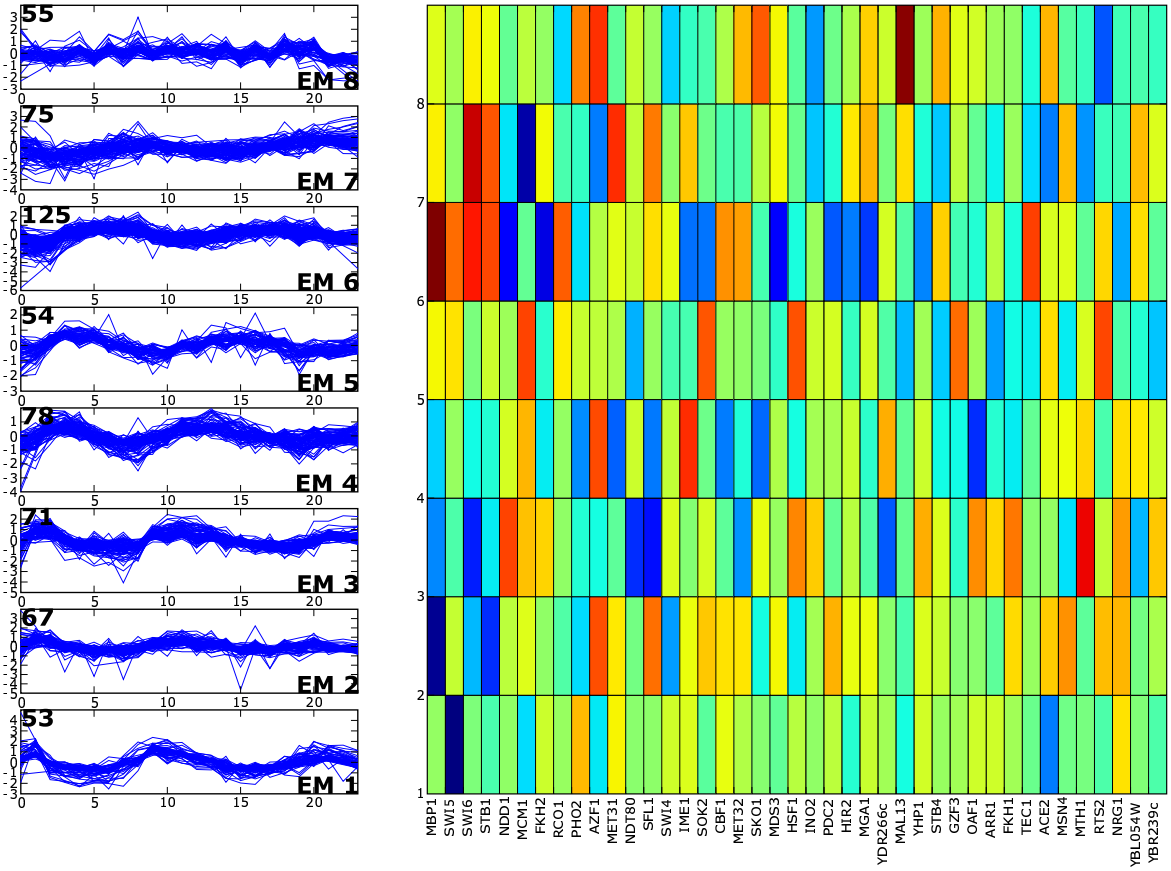

(a) Cdc15 ANN Weights, sorted by sum of squares

Figure 8

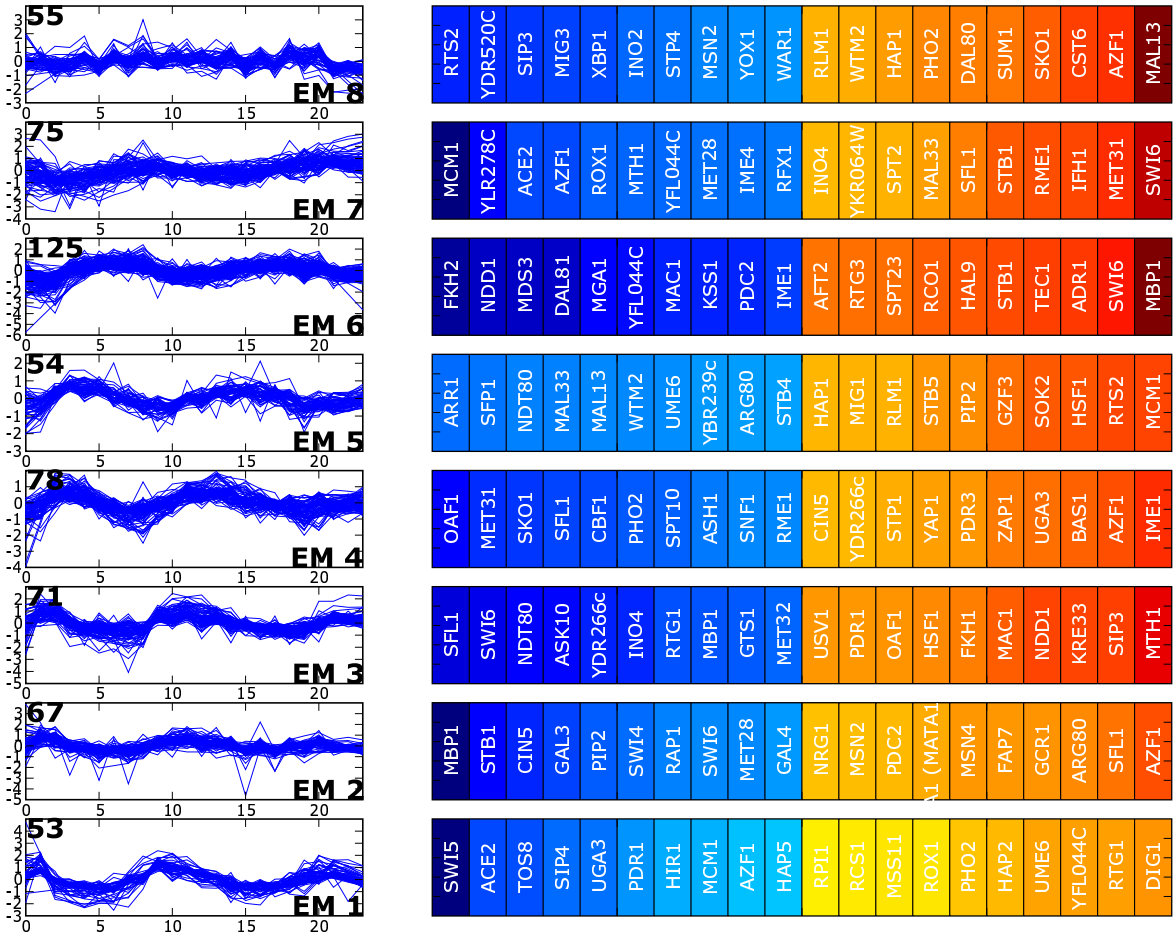

(b) Cdc15 ANN Weights, sorted by expression class weights

Figure 8

Figure 8: **Cdc15 ANN weights**. a) Shown are the ANN weights sorted by our sum-of-squares metric as in figure 3b. b) Shown are the ANN weights from the average-of-best network as in figure 5 for ANNs trained to predict RNA expression clusters derived from yeast cultures synchronized using Cdc15 TS mutant (Spellman et al., 1998)

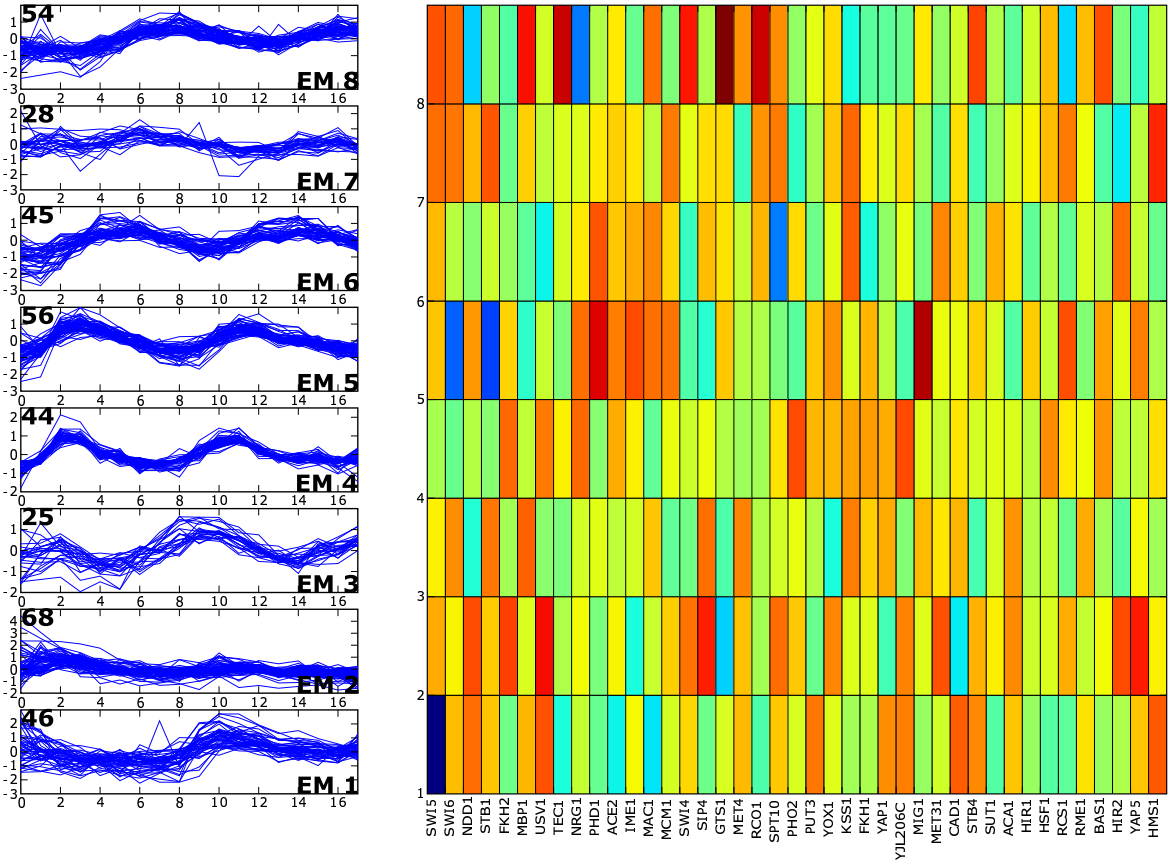

(a) Alpha ANN Weights, sorted by expression class weights

Figure 9

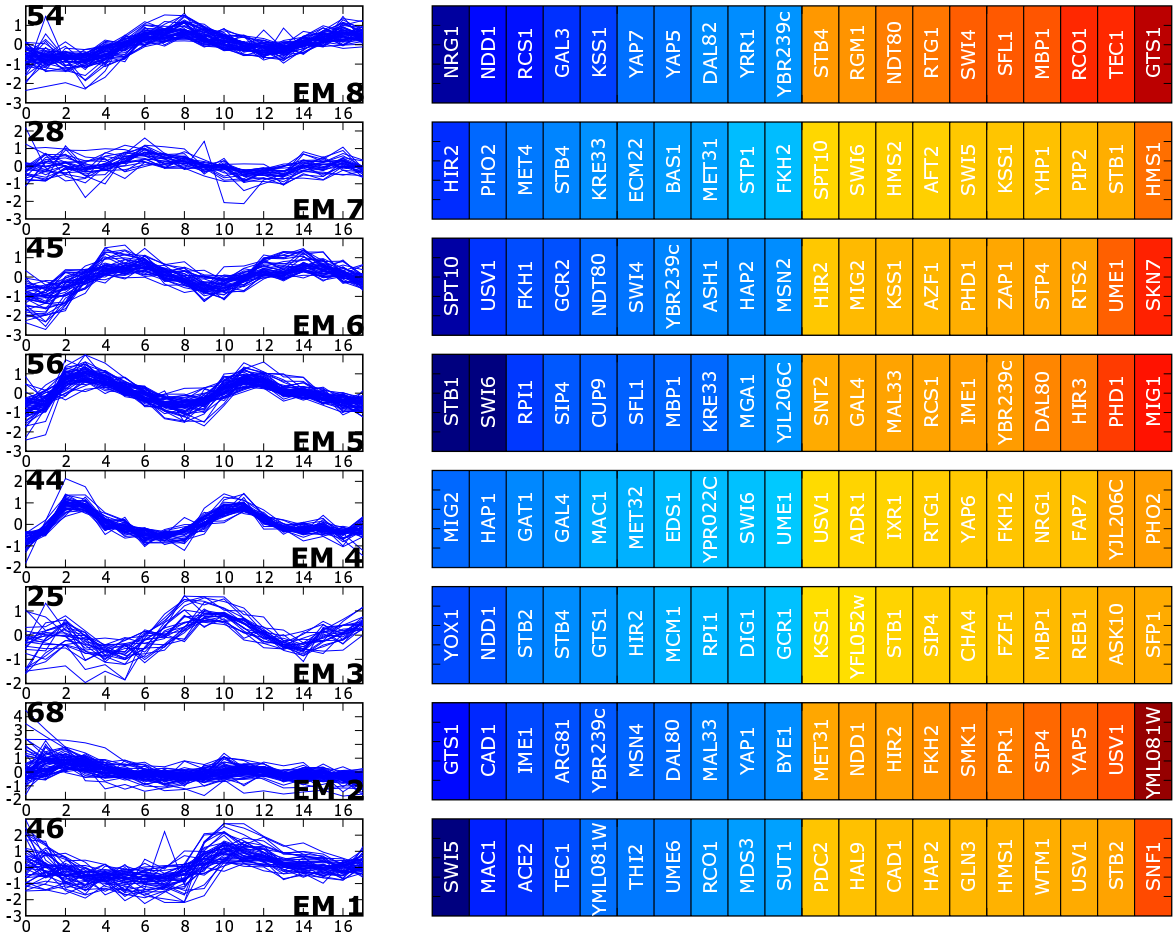

(b) Alpha ANN Weights, sorted by expression class weights

Figure 9

Figure 9: **Alpha Factor ANN weights**. a) Shown are the ANN weights sorted by our sum-of-squares metric as in figure 3b. b) Shown are the ANN weights from the average-of-best network as in figure 5 for ANNs trained to predict RNA expression clusters derived from yeast cultures synchronized using Cdc15 TS mutant (Spellman et al., 1998)

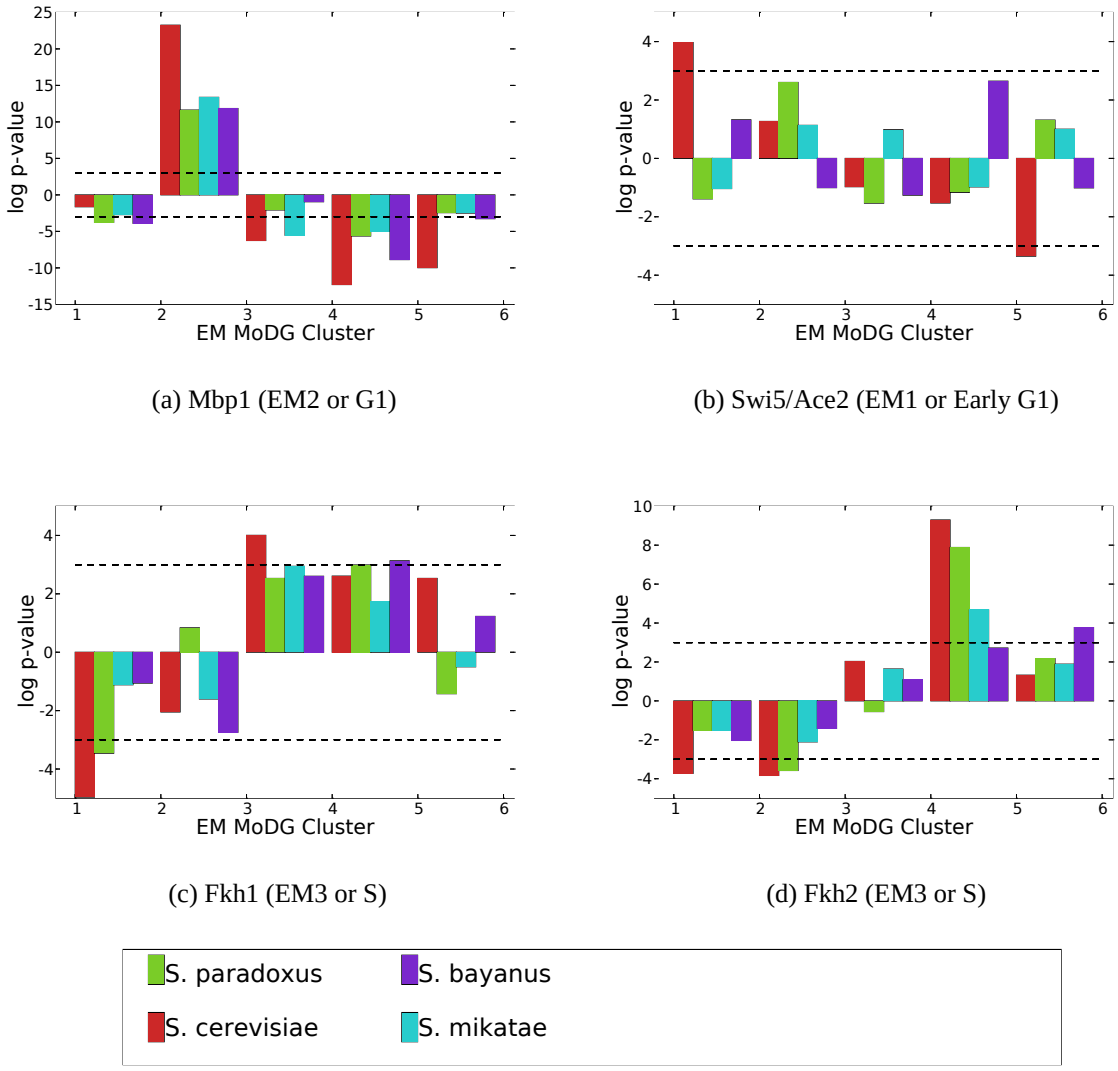

(a) Mbp1 (EM2 or G1)

(b) Swi5/Ace2 (EM1 or Early G1)

(c) Fkh1 (EM3 or S)

(d) Fkh2 (EM3 or S)

Figure 10: **Binding Site Enrichment and Depletion**. For several of the regulators highlighted by strong positive or negative association with particular expression classes (figure 5 and denoted pathetically) we calculated site enrichment p-values for each EM MoDG cluster across each of shown Saccharomyces species (see methods). Each p-value was calculated using only the cell cycle identified genes that were also used as input genes to the ANN. Each block of bars along the x-axis represent log p-values (y-axis) for a EM MoDG clusters. Each bar within these blocks are log p-value measurements for a different Saccharomyces species as indicated by the color legend. Enrichment is shown as positive values (-log p-values) and depletion is shown as negative values(log p-values). The species have been arranged by evolutionary distance from S. cerevisiae. From left to right: S. cerevisiae, S. paradoxus, S. mikatae, S. bayanus. A dashed line along the graphs at p-value = .05 has been drawn to help visualize the scale difference between the plots. a-d) enrichment bar charts for the specified binding sites, if the binding site is referred to by a name other than the regulator that binds to it, the regulators that bind are parenthetically shown. A displaying the color map used for each bar is shown at the bottom of the figure.

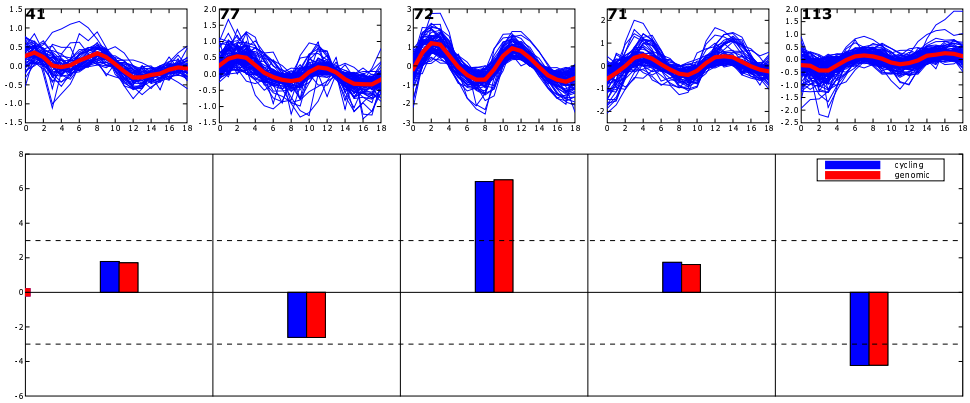

Figure 11: Binding Site Enrichment and Depletion for S. Pombe. Shown are the MCB enrichment p-values for S. pombe based an EM MoDG clustering of the expression data from (Rustici et al., 2004). Cluster summaries for each of the expression clusters are shown along the top panels, red lines are the mean expression trajectory and cluster sizes are in the upper left corner. Below is a bar chart of p-values. Shown are the p-values normalized against only the cycling genes (blue) and p-values normalized against the whole genome (red).

6 Supplemental Figures

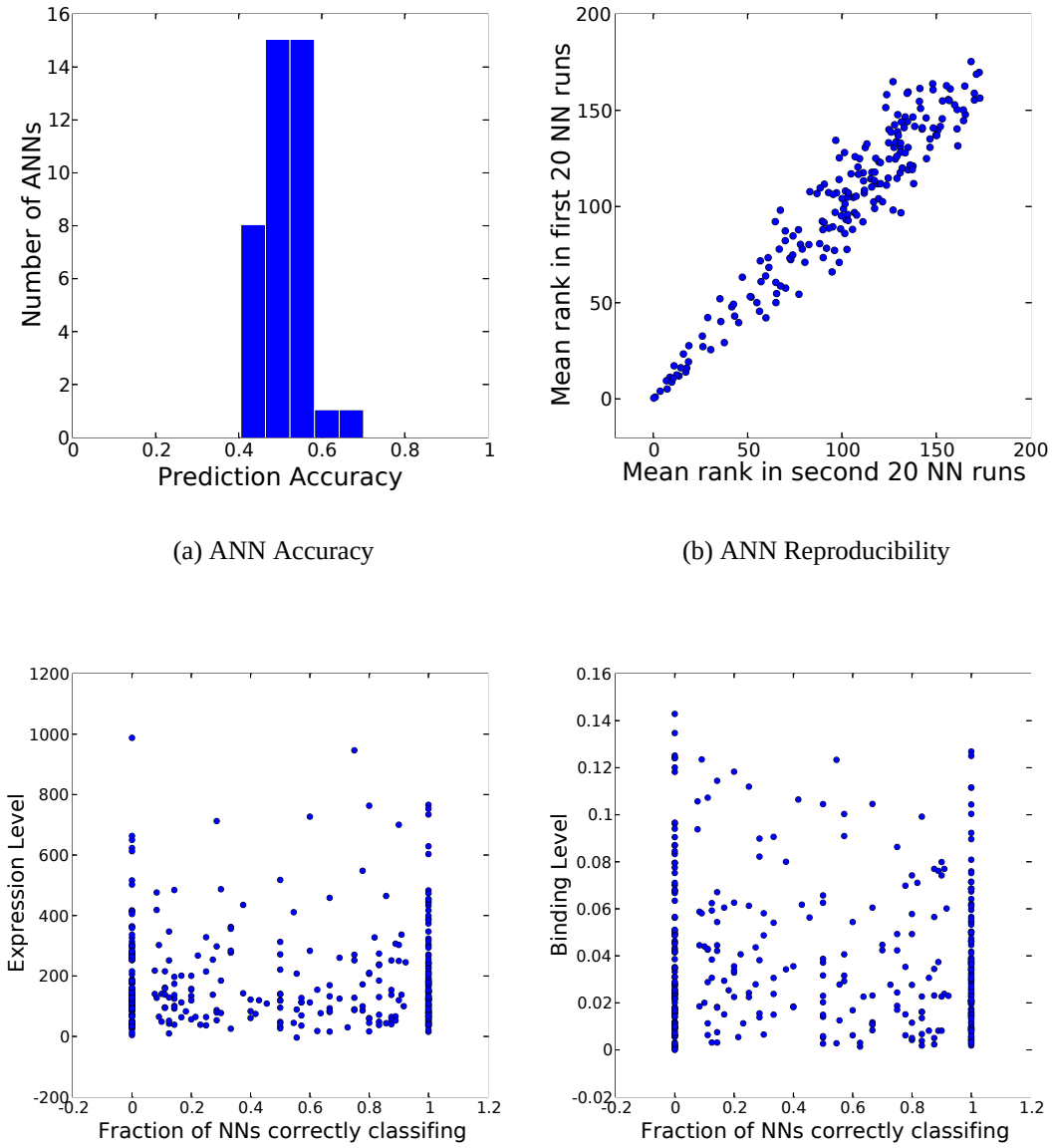

(a) ANN Accuracy

(b) ANN Reproducibility

(c) Predictability Vs Expression Level

(d) Predictability Vs Binding Level

Figure 1: **ANN Prediction Accuracy Histogram and correlations with binding and expression levels**. We trained 40 ANNs (see methods) to predict a gene expression behavior from only the regulator binding activity upstream to its start of transcription. For each network we trained on 80% of the data and tested on the remaining 20%. a) The distribution of ANN accuracy across the 40 trained ANNs. Along the x-axis are bins of accuracy ranges, the y-axis counts the number of ANNs that showed the designated prediction accuracy. b) Displays the relative reproducibility of the ANN rankings. Each regulator was ranked by its net influence in the ANN using a sum of squared weights metric across the classes in the weight matrix. Shown is a scatter plot of the regulator ranks from the first 20 ANNs vs the second 20 ANNs trained. c) Scatter plot of the predictability (fraction of ANNs correctly classifying a gene correctly) vs mean absolute expression level of the 4 highest measured time points for each gene. d) Predictability vs mean binding level for the 10 highest bound regulators.

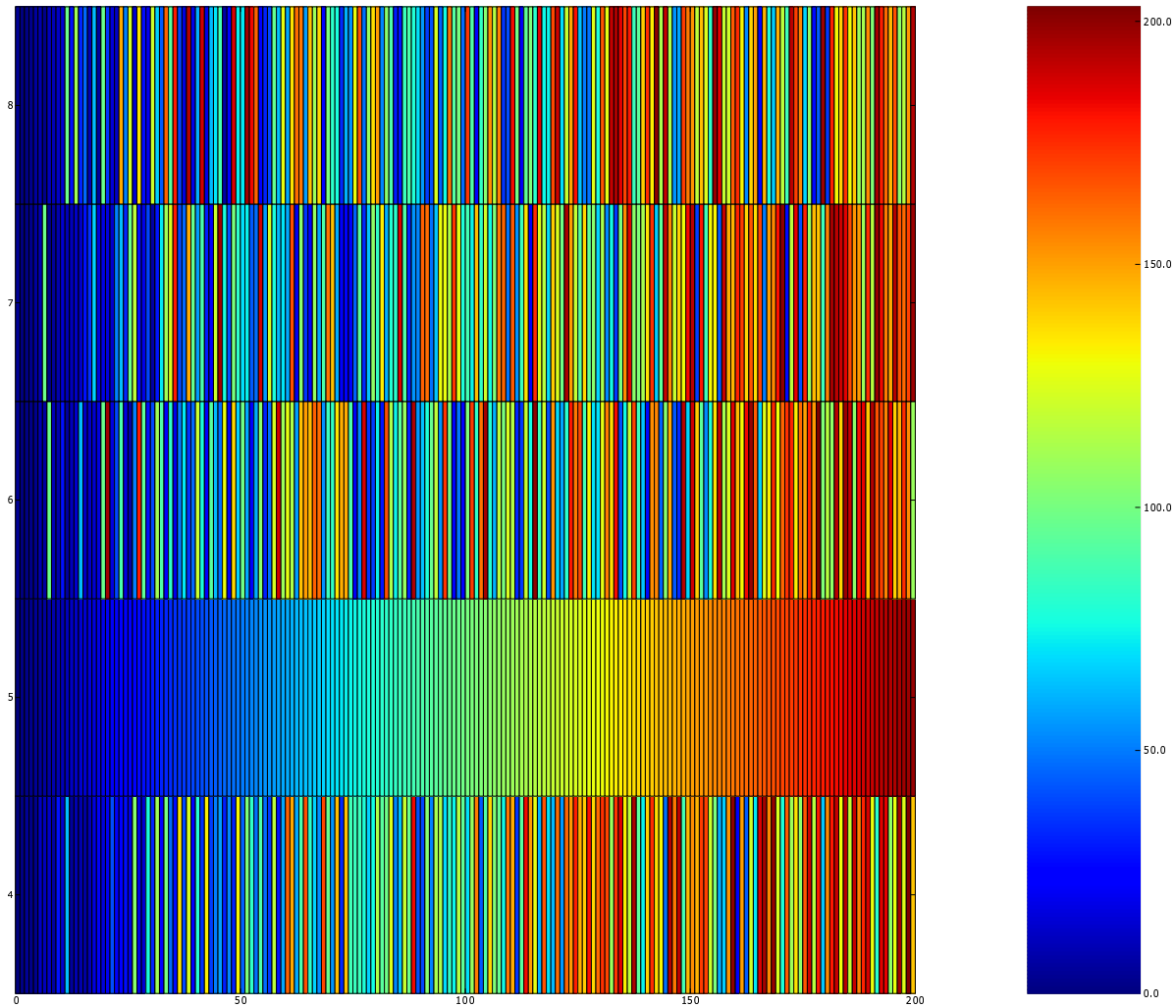

(a) Overview of network changes

Figure 2

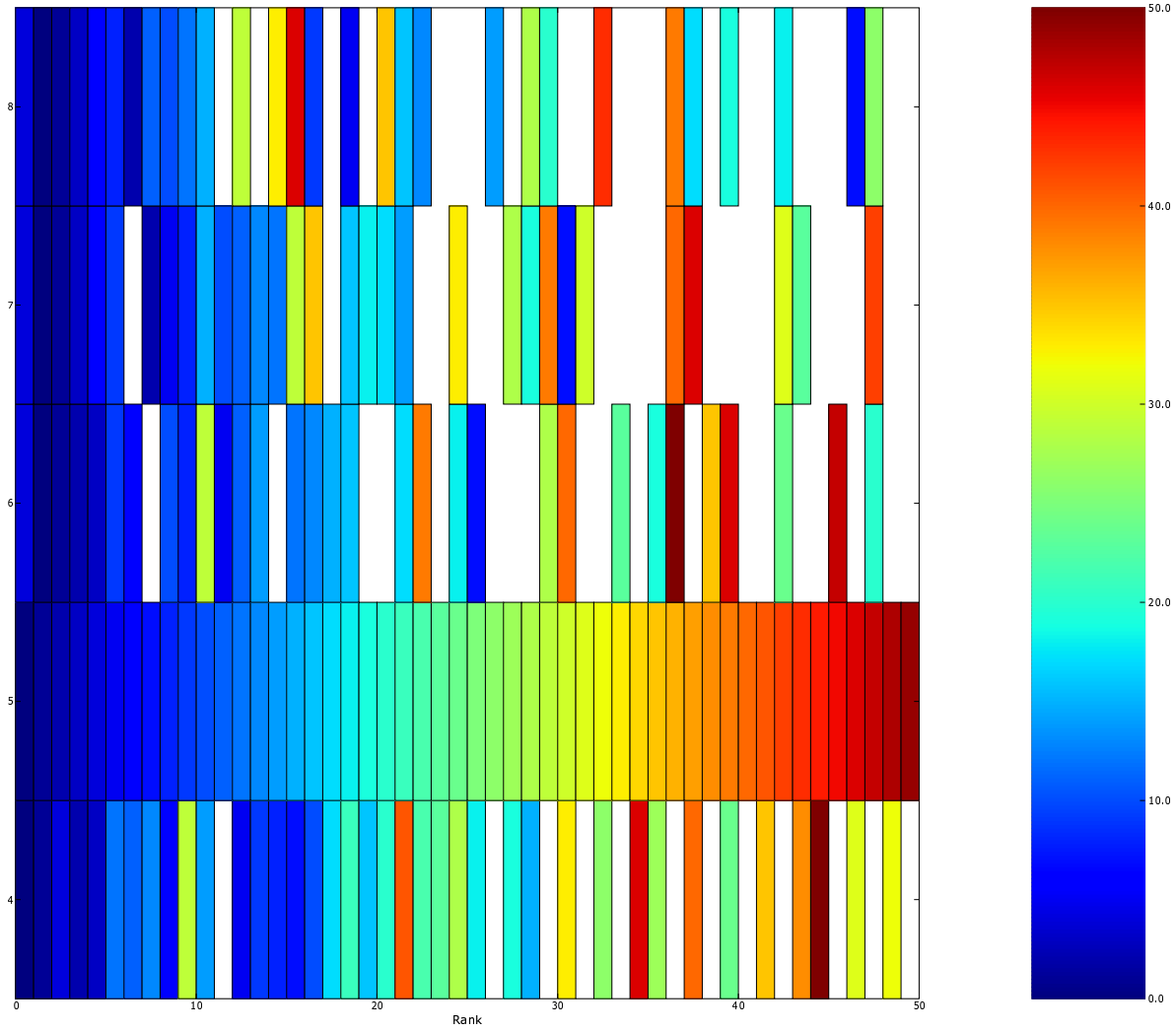

(b) Network changes for the top 50 regulators

Figure 2

Figure 2: **Network Ranks Across Varying Ks** Shown are results from training ANNs starting with a clustering composed of k=4,5,6,7 or 8 clusters. Within each heatmap each cell represents a regulator, the position of the cell along the x-axis of the plot is determined by the k-altered network, but the color is indicative of the regulator's rank in the k=5 network (as shown in figure 3). a) An overview showing the overall rank stability of the regulators across all mutant networks generated. b) A higher resolution view of the top ranked regulators for each mutant network. Only the top 50 regulators are shown, and the color spectrum is adjusted to only span 1-50. Any regulator that was ranked within the top 50 regulators in a mutant network, but not in the wildtype network is shown as white.

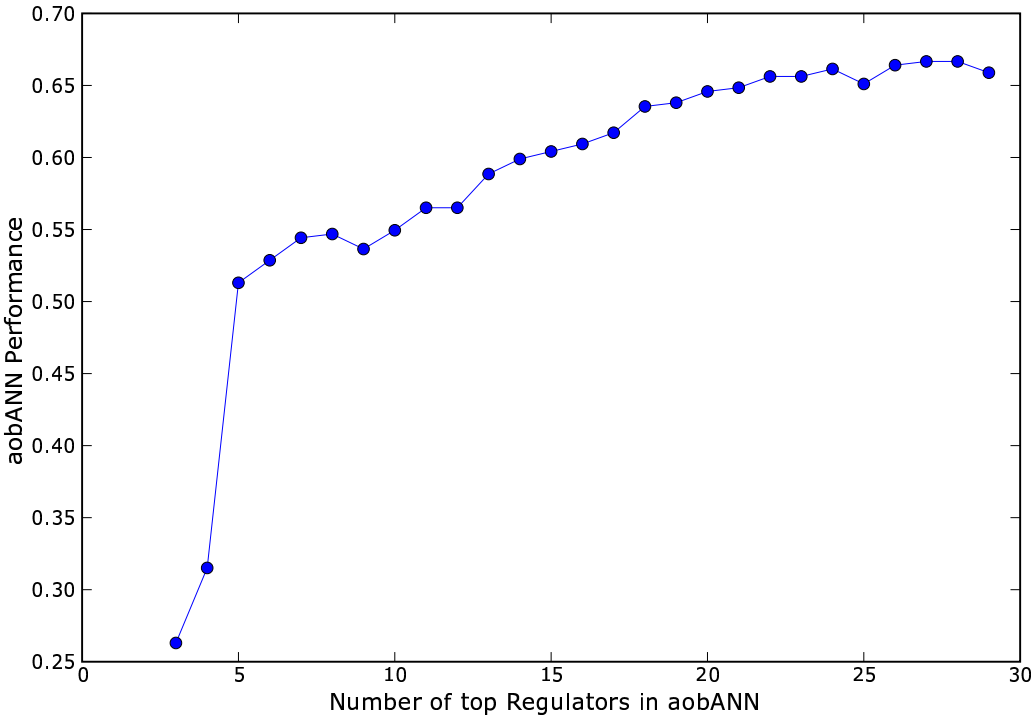

Figure 3: We trained aobANNs (see methods) using only the top 3-30 regulators. Plotted is the aobANN performance as a function of the number of top regulators included.

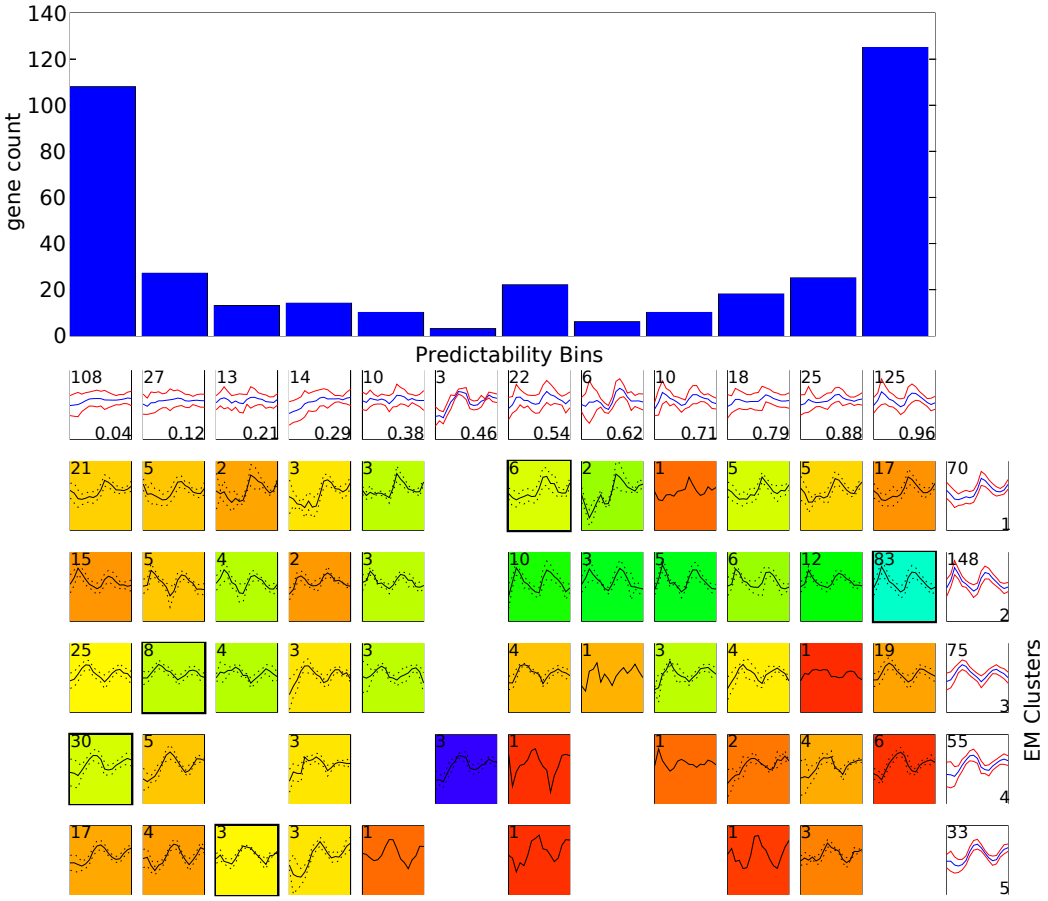

Figure 4: **Distribution of Neural Network Prediction Accuracy across EM MoDG Clusters**. The y-axis on the top panel measures the number of genes correctly classified by the indicated fraction of the trained ANNs (x-axis, bin range specified in the lower right corner of corresponding confusion array cells). Each bin is then broken up across the 5 EM MoDG clusters using a confusion array.

7 Table of Top regulators

Gene Descriptions for the top ten positively and negatively associated regulators for each cluster as determined by the ANN weights matrix figure 5. (Source http://www.yeastgenome.org)

Cluster	±	Regulator	Description
EM 1	+	SUT1	Involved in sterol uptake
	+	SWI5	transcriptional activator
	+	HAP5	Regulates respiratory functions; subunit of a heterotrimeric complex required for CCAAT binding
	+	ACE2	involved in transcriptional regulation of CUP1. enters nucleus only at the end of mitosis.
	+	RTS2	similar to mouse KIN7 protein
	+	DAL80	Negative regulator of multiple nitrogen catabolic genes
	+	TEC1	transcription factor of the TEA/ATTS DNA-binding domain family, regulator of Ty1 expression
	+	AZF1	probable transcription factor, suppressor of mutation in the nuclear gene for the core subunit of mitochondrial RNA polymerase
	+	YFL044C	None
	+	MOT3	DNA-binding protein implicated in heme-dependent repression, repression of a subset of hypoxic genes by Rox1p, repression of several DAN/TIR genes during aerobic growth, and regulation of membrane-related genes
	-	NDD1	Nuclear Division Defective 1
	-	YJL206C	None
	-	HAP2	Global regulator of respiratory genes
	-	STB4	binds Sin3p in two-hybrid assay
	-	GLN3	Responsible for nitrogen catabolite repression (NCR)-sensitive transcription. During nitrogen starvation, Gln3 is nuclear. Under excess nitrogen, Gln3 is cytoplasmic. Also regulates glutamine-repressible gene products.
	-	YAP3	bZIP protein; transcription factor
	-	WAR1	
	-	SFL1	Transcription factor with domains homologous to myc oncoprotein and yeast Hsf1p required for normal cell surface assembly and flocculence
	-	CAD1	Transcriptional activator involved in resistance to 1,10-phenanthroline; member of yeast Jun-family of transcription factors related to mammalian c-jun
	-	PHO2	Regulation of phosphate metabolism

Cluster	±	Regulator	Description
EM 2	+	SWI6	Involved in cell cycle dependent gene expression
	+	MBP1	transcription factor
	+	STB1	binds Sin3p in two-hybrid assay and is present in a large protein complex with Sin3p and Stb2p
	+	SFL1	Transcription factor with domains homologous to myc oncoprotein and yeast Hsf1p required for normal cell surface assembly and flocculence
	+	WTM1	WD repeat containing transcriptional modulator 1
	+	LEU3	Regulates genes involved in branched chain amino acid biosynthesis and in ammonia assimilation. Positively regulated by alpha-isopropylmalate, an intermediate in leucine biosynthesis.
	+	GAT1	activator of transcription of nitrogen-regulated genes; inactivated by increases in intracellular glutamate levels
	+	YPR196W	None
	+	HAP3	Regulates respiratory functions; encodes divergent overlapping transcripts
	+	NDT80	Meiosis-specific gene; mRNA is sporulation specific; required for exit from pachytene and for full meiotic recombination
	-	FKH2	Fork Head homolog two
	-	NRG1	involved in regulation of glucose repression
	-	PUT3	Positive regulator of PUT (proline utilization) genes
	-	USV1	None
	-	NDD1	Nuclear Division Defective 1
	-	YOX1	Homeodomain protein that binds leu-tRNA gene. acts as a repressor at early cell cycle boxes (ECBs) to restrict their activity to the M/G1 phase of the cell cycle.
	-	MIG3	
	-	UME6	Regulator of both repression and induction of early meiotic genes. Ume6p requires Ume4 for mitotic repression and interacts with and requires Ime1p and Rim11p for induction of meiosis-specific transcription
	-	SMP1	Second MEF2-like Protein 1 Transcription factor of the MADS (Mcm1p, Agamous, Deficiens, SRF) box family; closely related to RLM1
	-	ARO80	

Cluster	±	Regulator	Description
EM 3	+	FKH1	forkhead protein
	+	PUT3	Positive regulator of PUT (proline utilization) genes
	+	FKH2	Fork Head homolog two
	+	USV1	None
	+	ARR1	Similar to transcriptional regulatory elements YAP1 and cad1
	+	RLM1	serum response factor-like protein that may function downstream of MPK1 (SLT2) MAP-kinase pathway
	+	YKL222C	None
	+	WTM2	WD repeat containing transcriptional modulator 2
	+	BYE1	
	+	MAL33	Part of complex locus MAL3; nonfunctional in S288C, shows homology to both functional & nonfunctional MAL-activator proteins in other Sc strains & to other nonfunctional MAL-activator sequences from S288C (i.e. MAL33, YPR196W, & YFL052W)
	-	WTM1	WD repeat containing transcriptional modulator 1
	-	ACE2	involved in transcriptional regulation of CUP1. enters nucleus only at the end of mitosis.
	-	ARG81	Regulator of arginine-responsive genes with ARG80 and ARG82
	-	IFH1	Interacts with fork head protein. Protein controlling pre-rRNA processing machinery in conjunction with Fhl1p
	-	SMK1	SMK1 encodes a mitogen-activated protein kinase required for spore morphogenesis that is expressed as a middle sporulation-specific gene.
	-	RPI1	possesses a transcriptional activation domain and affects the mRNA levels of several cell wall metabolism genes.
	-	HAP4	Regulates respiratory functions; encodes divergent overlapping transcripts
	-	INO2	Transcription factor required for derepression of inositol-choline-regulated genes involved in phospholipid synthesis
	-	SFL1	Transcription factor with domains homologous to myc oncoprotein and yeast Hsf1p required for normal cell surface assembly and flocculence
	-	RAP1	DNA-binding protein involved in either activation or repression of transcription, depending on binding site context. Also binds telomere sequences and plays a role in telomeric position effect (silencing) and telomere structure.

Cluster	±	Regulator	Description
EM 4	+	NDD1	Nuclear Division Defective 1
	+	DAL81	Positive regulator of multiple nitrogen catabolic genes
	+	ACA1	contains an ATF/CREB-like bZIP domain; transcriptional activator
	+	PDC2	Regulates transcription of PDC1 and PDC5, which encode pyruvate decarboxylase
	+	FKH2	Fork Head homolog two
	+	IME4	IME4 appears to activate IME1 in response to cell-type and nutritional signals and thereby regulate meiosis
	+	MBF1	
	+	WAR1	
	+	INO4	Transcription factor required for derepression of inositol-choline-regulated genes involved in phospholipid synthesis
	+	UME6	Regulator of both repression and induction of early meiotic genes. Ume6p requires Ume4 for mitotic repression and interacts with and requires Ime1p and Rim11p for induction of meiosis-specific transcription
	-	SWI6	Involved in cell cycle dependent gene expression
	-	GAT1	activator of transcription of nitrogen-regulated genes; inactivated by increases in intracellular glutamate levels
	-	FAP7	
	-	MAC1	metal-binding transcriptional activator
	-	YAP6	bZIP protein
	-	HIR1	Involved in cell-cycle regulation of histone transcription
	-	HAP5	Regulates respiratory functions; subunit of a heterotrimeric complex required for CCAAT binding
	-	TEC1	transcription factor of the TEA/ATTS DNA-binding domain family, regulator of Ty1 expression
	-	SWI5	transcriptional activator
	-	MBP1	transcription factor

Cluster	±	Regulator	Description
EM 5	+	YOX1	Homeodomain protein that binds leu-tRNA gene. acts as a repressor at early cell cycle boxes (ECBs) to restrict their activity to the M/G1 phase of the cell cycle.
	+	MCM1	Involved in cell-type-specific transcription and pheromone response
	+	FAP7	
	+	CRZ1	calcineurin responsive zinc-finger
	+	NRG1	involved in regulation of glucose repression
	+	HAP5	Regulates respiratory functions; subunit of a heterotrimeric complex required for CCAAT binding
	+	PHO4	Transcription factor that activates expression of phosphate pathway
	+	YDR049W	None
	+	PHD1	protein similar to StuA of Aspergillus nidulans
	+	SPT23	Dosage dependent suppressor of Ty-induced promoter mutations. Homolog of Mga2. Spt23p and Mga2p differentially activate and regulate OLE1 transcription.
	-	HMS1	High-copy mep2 suppressor
	-	SWI6	Involved in cell cycle dependent gene expression
	-	HSF1	heat shock transcription factor
	-	LEU3	Regulates genes involved in branched chain amino acid biosynthesis and in ammonia assimilation. Positively regulated by alpha-isopropylmalate, an intermediate in leucine biosynthesis.
	-	STP2	Involved in pre-tRNA splicing and in uptake of branched-chain amino acids
	-	BAS1	Transcription factor regulating basal and induced activity of histidine and adenine biosynthesis genes
	-	MAL13	Part of complex locus MAL1; nonfunctional in S288C, shows homology to both functional & nonfunctional MAL-activator proteins in other Sc strains & to other nonfunctional MAL-activator sequences from S288C (i.e. MAL33, YPR196W, & YFL052W)
	-	HIR3	Involved in cell-cycle regulation of histone transcription
	-	UME6	Regulator of both repression and induction of early meiotic genes. Ume6p requires Ume4 for mitotic repression and interacts with and requires Ime1p and Rim11p for induction of meiosis-specific transcription
	-	PPR1	Positive regulator of URA1 and URA3

Table 2: